KNS 26 spring, Jeju, Korea
May 6-8, 2026

Numerical Evaluation of Displacement-Robust and Fault-Tolerant Four-Sensor Probe Arrays for Local Bubble Parameter Measurement in Two-Phase Flow

May 8, 2026

Minhong Cho, Xuan Quyet Do, Jinyeong Bak, Jae Jun Jeong, Byongjo Yun*

Department of Mechanical Engineering, Pusan National University

I. Introduction

- Importance of measuring local bubble parameters
  - Two-phase flow is a key phenomenon in nuclear thermal-hydraulic systems
  - Interfacial transfer terms depend on bubble parameters (Two-fluid model)
    - Void fraction (α), bubble velocity (v_g), interfacial area concentration (IAC, a_i), bubble diameter (d_b)
  - Accurate local bubble parameter data are essential for model development and validation

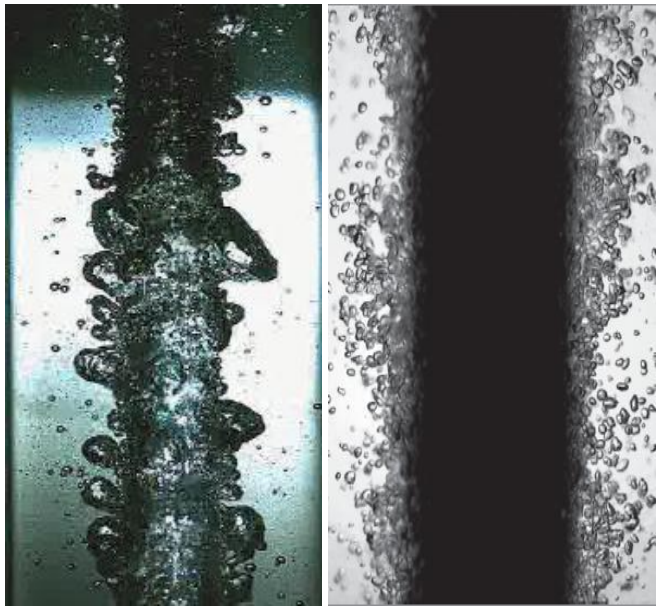

◎ **Bubble behavior under the boiling condition**

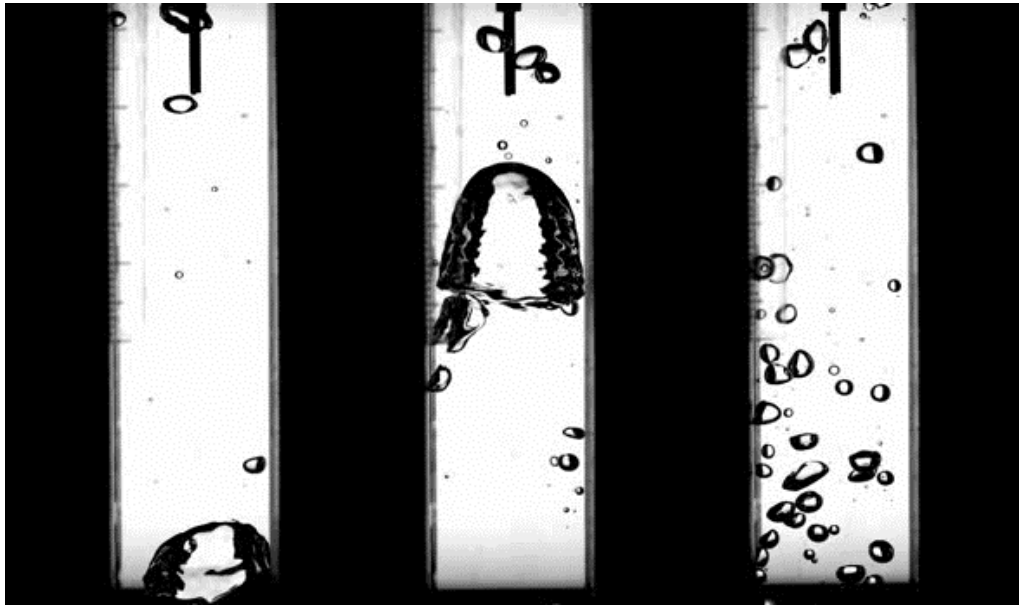

◎ **Measurement of bubbles using OFP sensor**

I. Introduction

- Optical fiber probe sensor (OFP)
  - Working principle
    - Phase detection by refractive-index difference
    - Back-scattered light intensity → voltage signal
  - Applicability and characteristics
    - Electrically non-conducting fluid / Fast response (> 500kHz)
    - High-temperature applicability (< 350˚C)

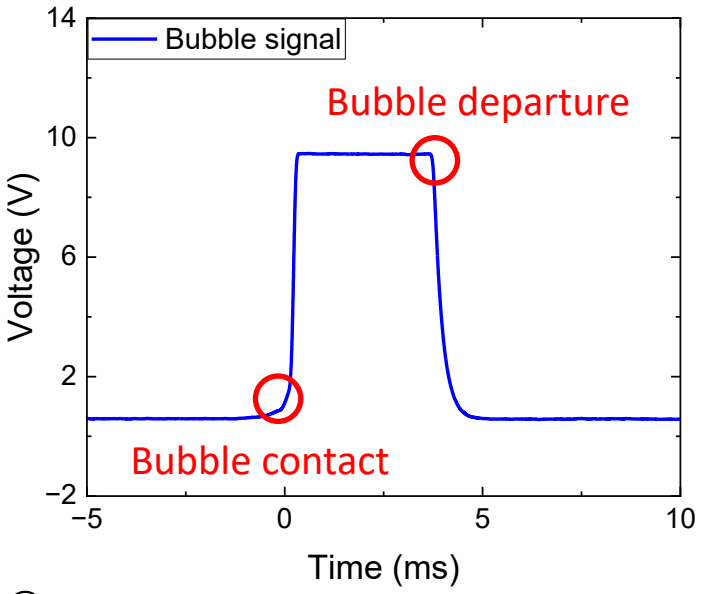

◎ **Typical bubble signal measured from OFP**

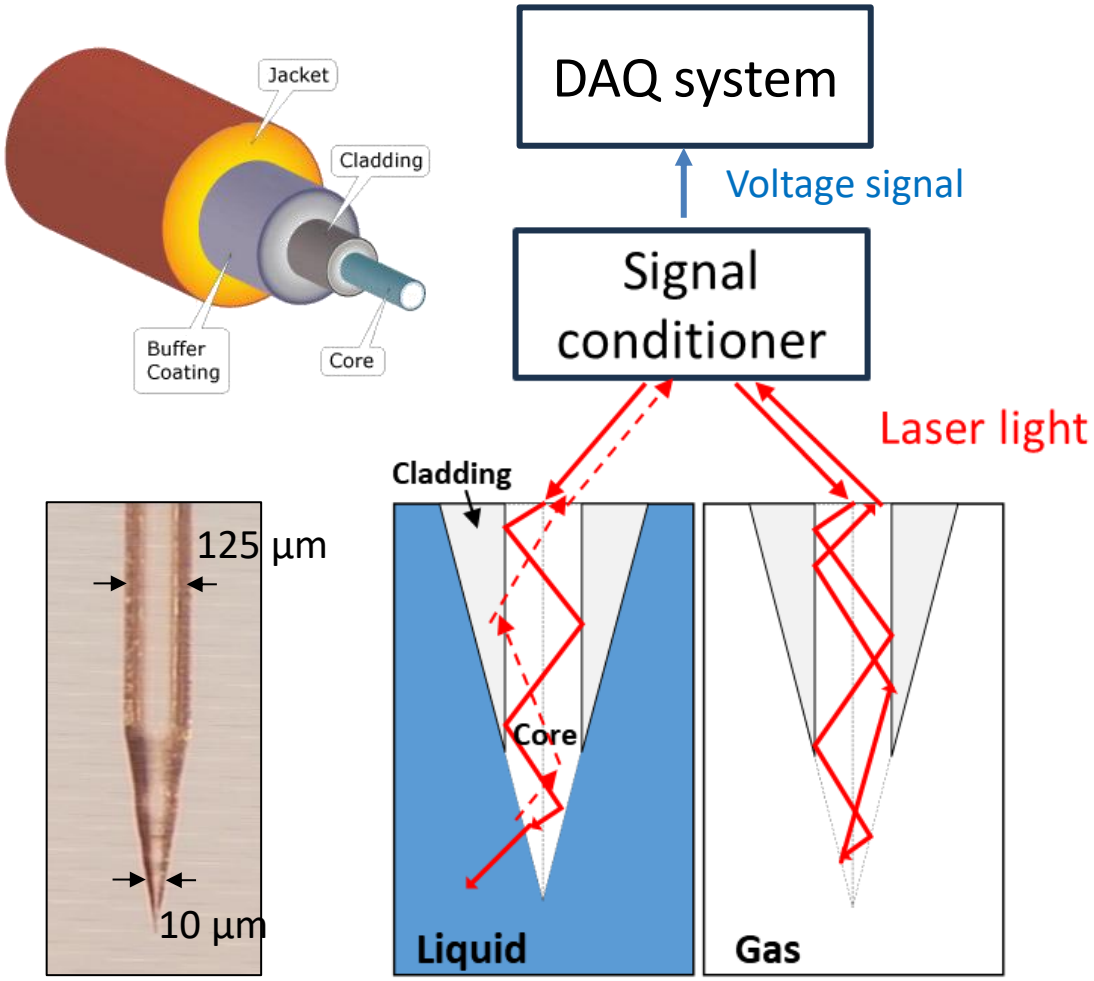

◎ **Optical fiber sensor** ◎ **Working principle of optical fiber sensor**

I. Introduction

◆ Bubble detection using a 4-sensor OFP

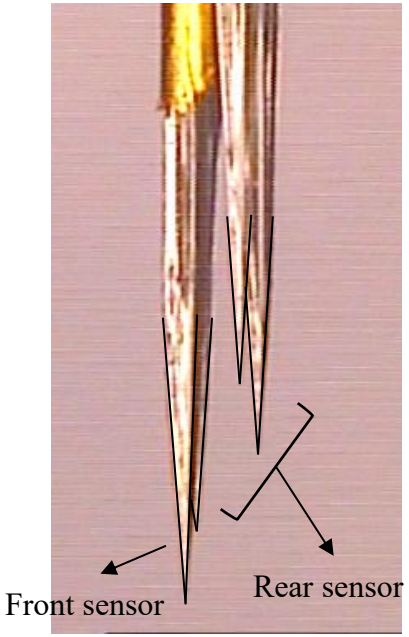

◎ 4-s optical fiber probe

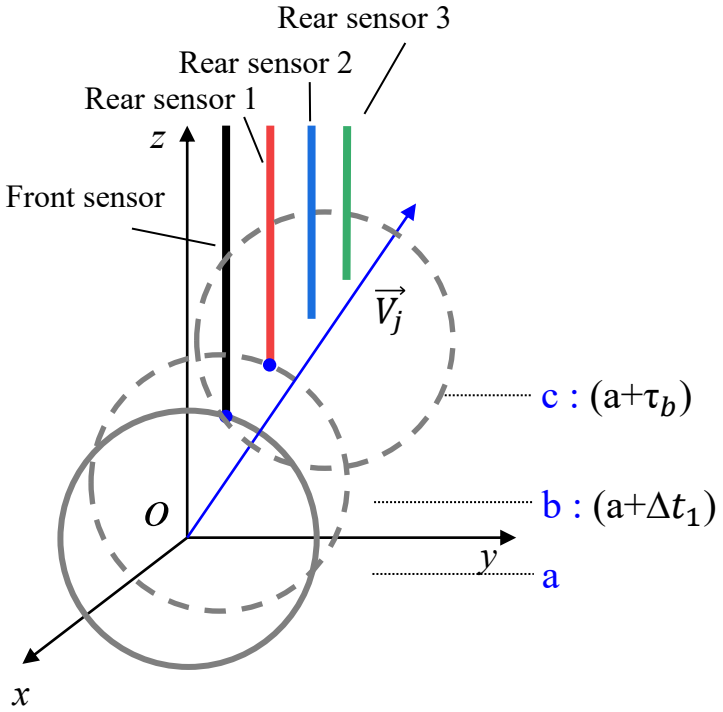

◎ Schematic of bubble measurement using 4-s OFP

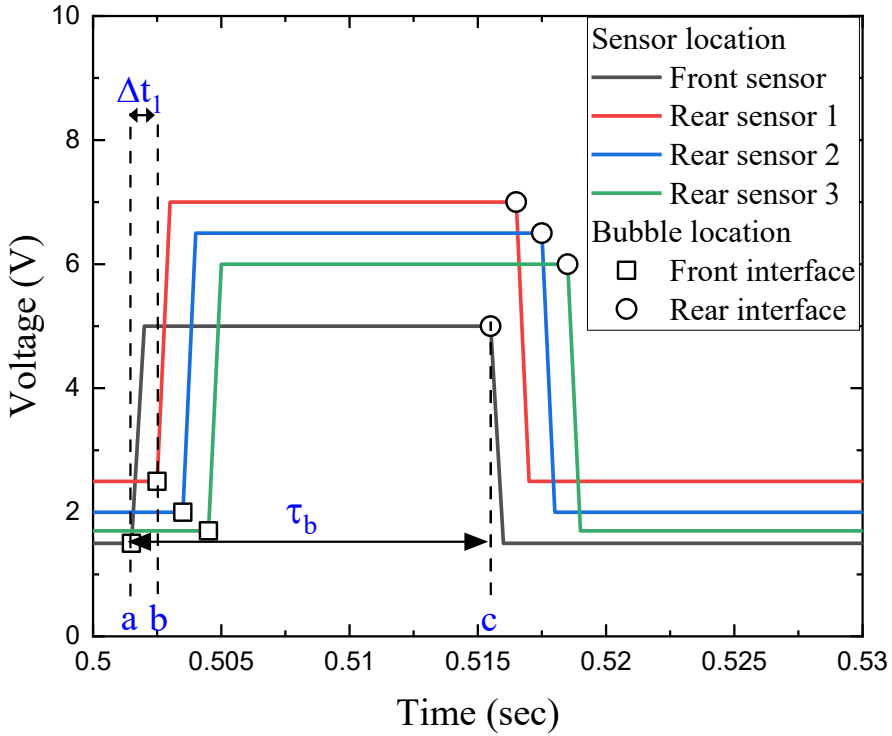

◎ Bubble signal measured from 4-s OFP

I. Introduction

◆ Calculation of the Bubble velocity (V_b)

❖ 1 pair of front-rear sensor

- 1-D velocity
- $V_{2-sensor} = \frac{\Delta z}{\Delta t}$

❖ 3 pair of front-rear sensor

- 3-D velocity vector

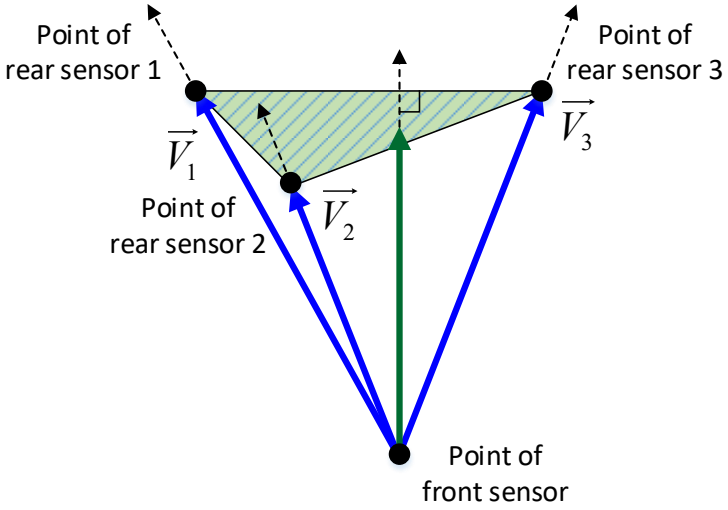

◎ **Schematic diagram of velocity vector**

◆ Measurement of Void fraction (α)

❖ $\alpha = \frac{\text{Total bubble residence time}}{\text{Total measuring time}} = \frac{\sum \tau_b}{t_{total}}$

◆ Calculation of Sauter mean diameter (D_{32})

❖ Interfacial area concentration (IAC, a_i)

- a_i = interfacial area/unit volume
- $\overline{a_i} \propto \frac{1}{\Omega}\sum_{j=1}^{N_{eff}} \left|\frac{1}{\vec{V}_{normal}}\right|$
- $D_{32} = \frac{6\alpha}{\overline{a_i}}$

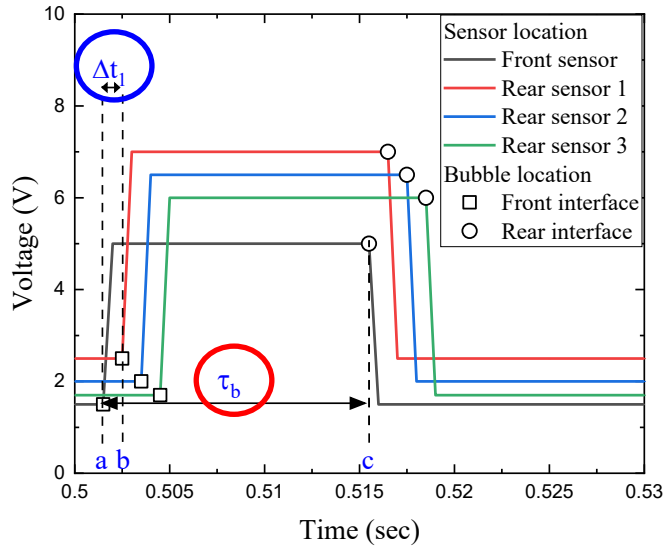

◎ **Bubble signal measured from 4-s OFP**

I. Introduction

◆ Limitation of coplanar 4-sensor configuration

❖ Damaged OFP in high-temperature water (over 300℃) conditions

- Penetration of high-temperature water into coating interface
- Degradation of the sensor tip may occur

➢ Sensor-tip displacement or signal loss may occur

❖ If front sensor is not working, bubble parameters cannot be measured

- $V = \frac{\Delta z}{\Delta t} \rightarrow \boldsymbol{\Delta z = 0}$

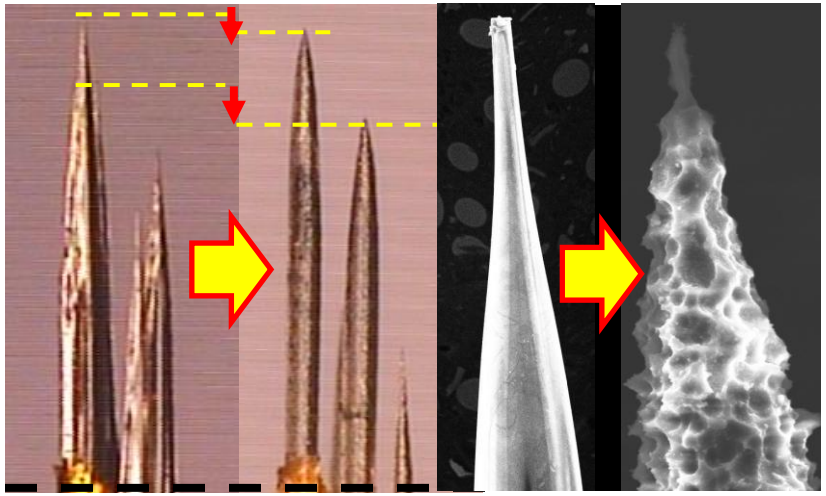

◎ Damaged optical fiber probes in the high temperature water

◆ Objective

❖ Evaluation of displacement-robust and fault-tolerant 4-sensor probe configurations

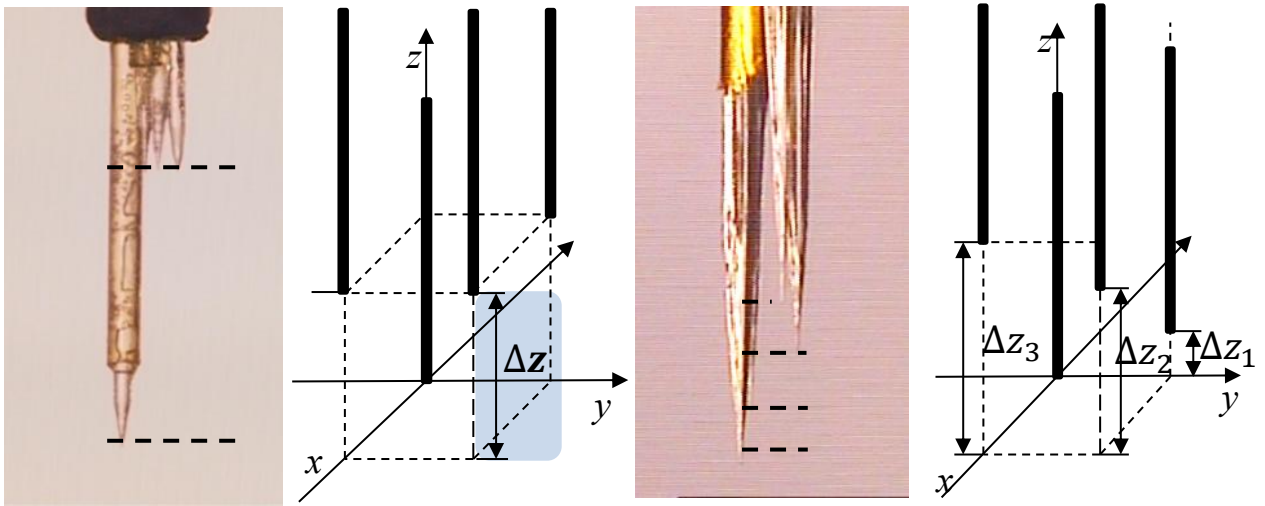

◎ Configurations of the 4-sensor probes : coplanar (left) and new (right)

II. Proposal of New 4-s configurations and Evaluation Method

◆ Setup of evaluated 4-sensor probe configurations

❖ Axial spacings between front-rear sensors ($\Delta z_k, k = 1,2,3$)

- $4^3 - 3^3 = 37$ configurations were evaluated

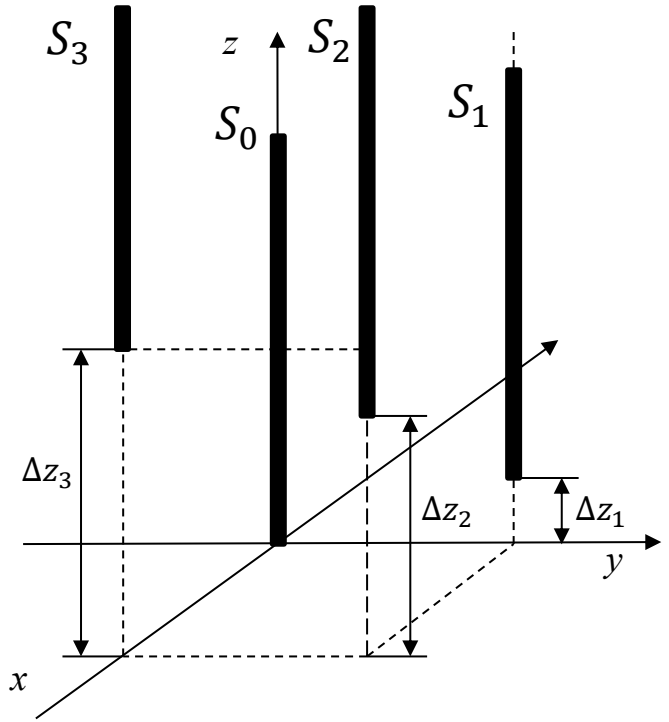

◎ **Configuration of the 4-sensor probes**

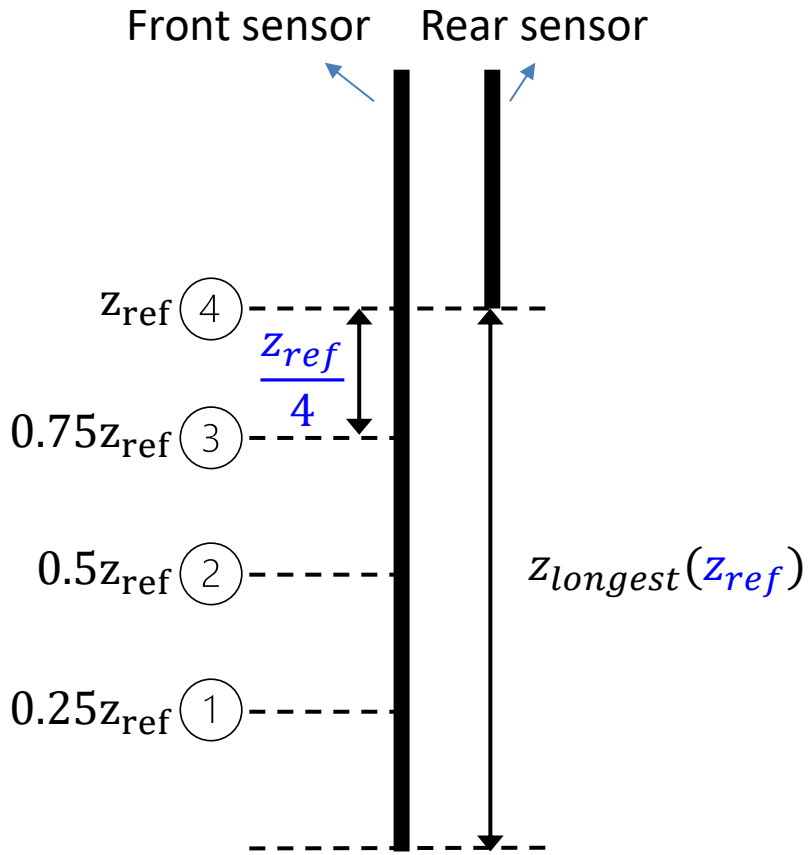

◎ **Normalized axial spacing between front-rear sensor**

II. Proposal of New 4-s configurations and Evaluation Method

◆ Monte-Carlo simulation

Generate bubble (V_b, D_b)

Simulate bubble-sensor contact

Extract Δt_1, Δt_2, Δt_3

Compare input and output value

Calculate V_b, IAC, D_{32}

4-sensor configuration

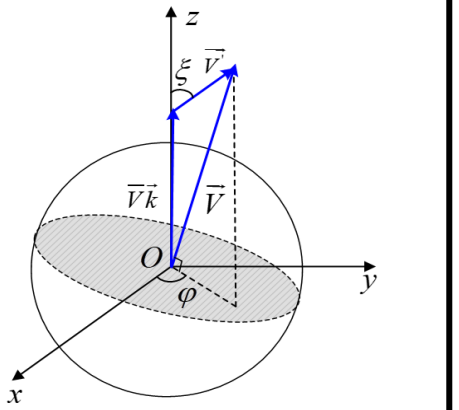

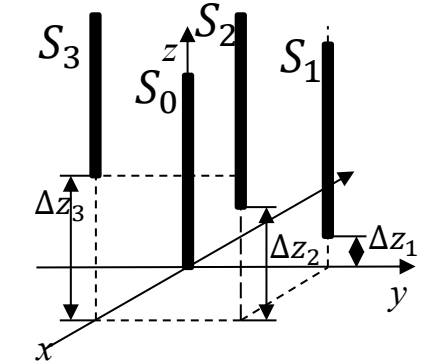

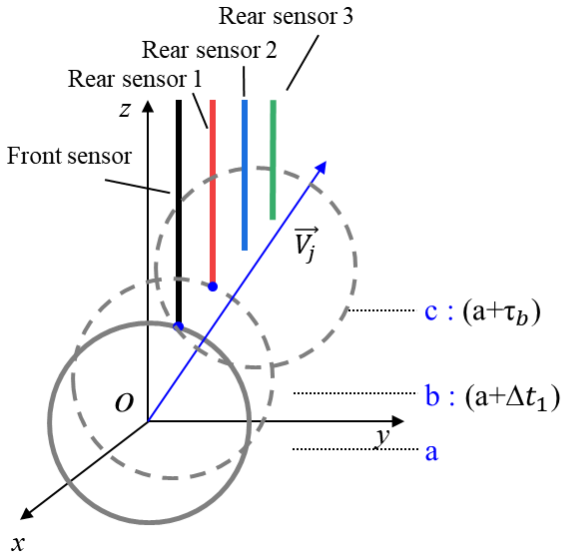

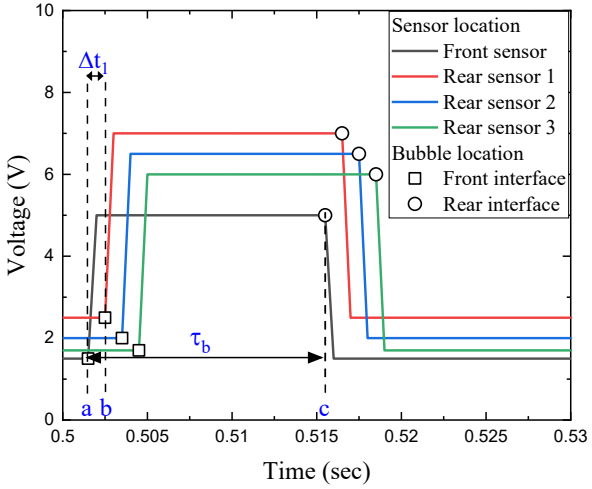

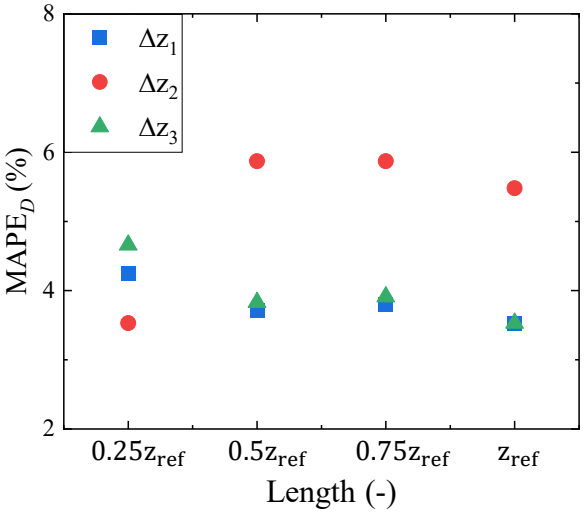

II. Proposal of New 4-s configurations and Evaluation Method

◆ Specifying flow conditions

❖ Input parameters for Monte Carlo simulation

- Fixed Bubble velocity ($\bar{V}$)
  - Scale of velocity only changes time scale ($V = \frac{\Delta z}{\Delta t}$)
  - No Δt error in simulation
- Maximum fluctuation ratio(H_{max}) : $H = \frac{|\bar{V}'|}{\bar{V}}$
  - $H_{max} = 0.0, 0.2$
- Bubble diameter(D_{30})
  - $D^* = \frac{D_{30}}{z_{ref}} = 0.1 \sim 5.0$
- Aspect ratio ($\beta = \frac{c}{a}$) : 1
- Bubble number : 250,000/case

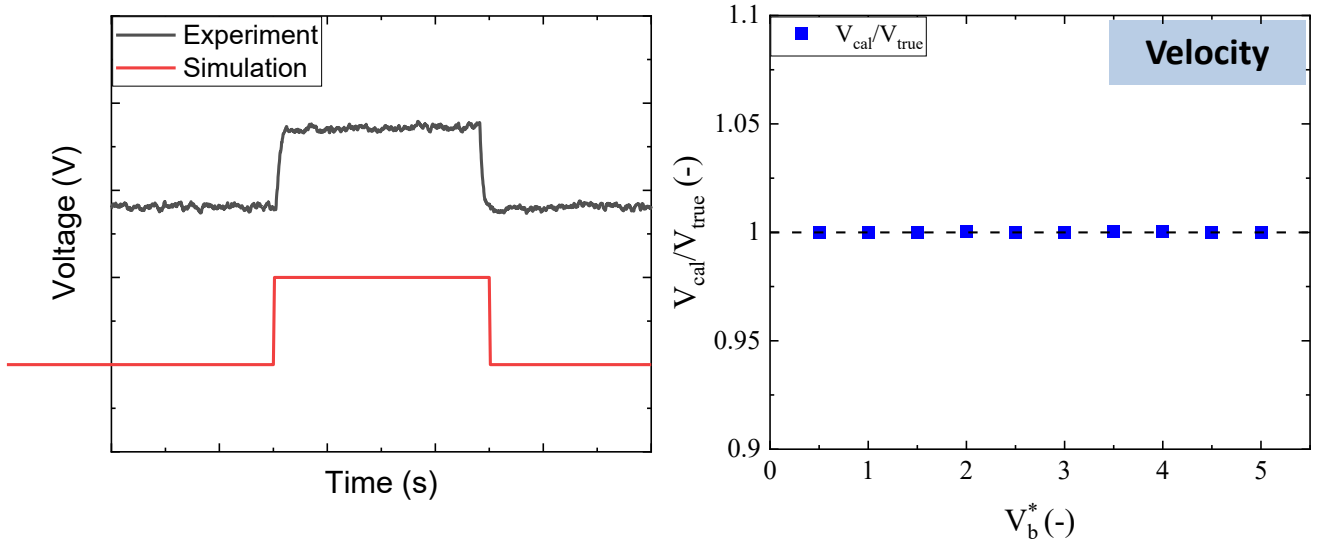

◎ Effect of bubble velocity in Monte-Carlo simulation

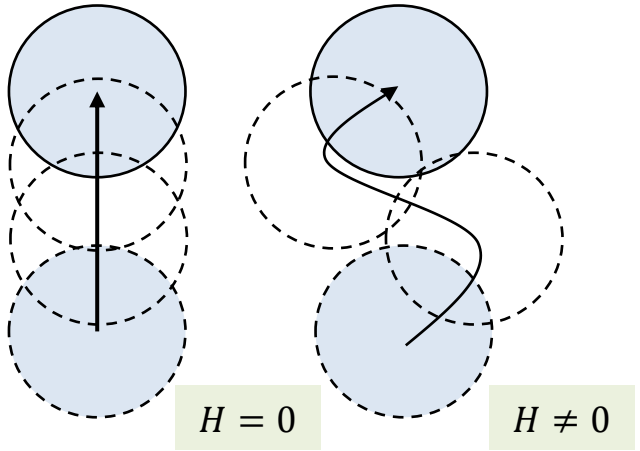

◎ Bubble movement with fluctuation

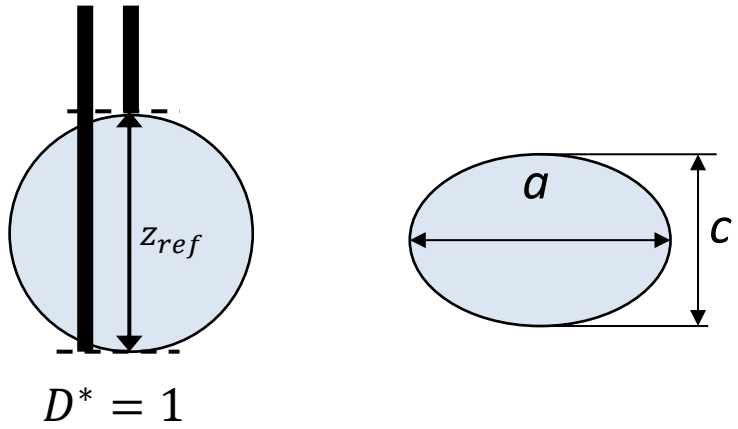

◎ Normalized bubble diameter and bubble shape

III. Evaluation results

◆ Measurement accuracy of bubble velocity(V_b)

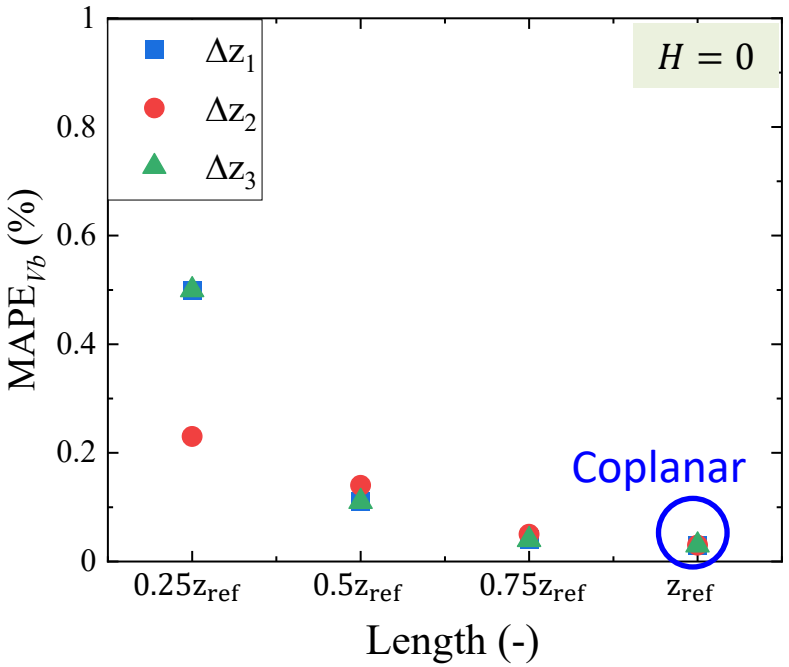

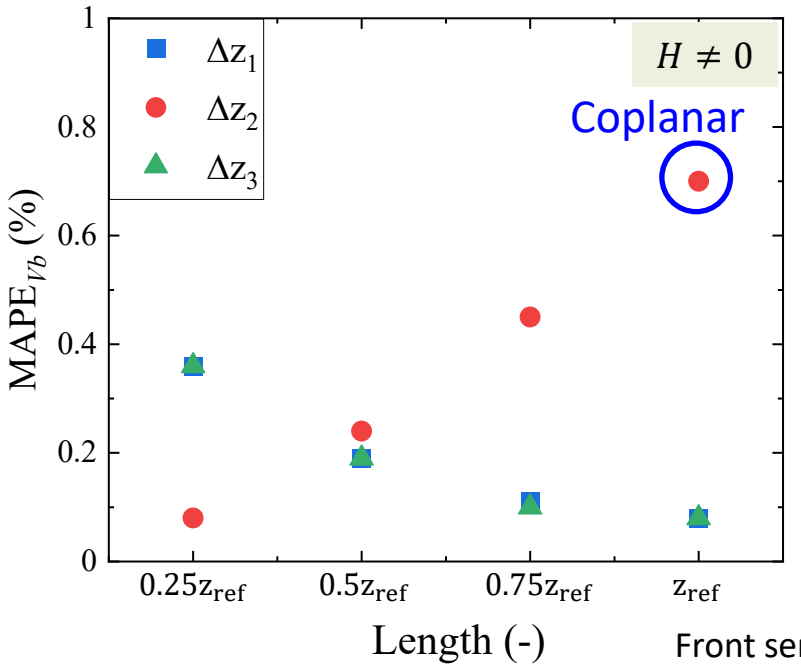

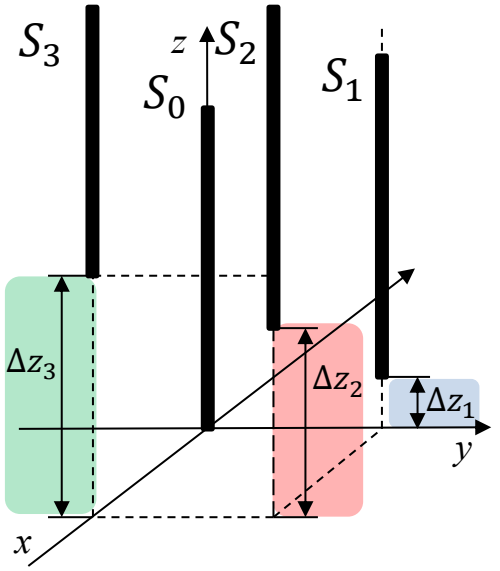

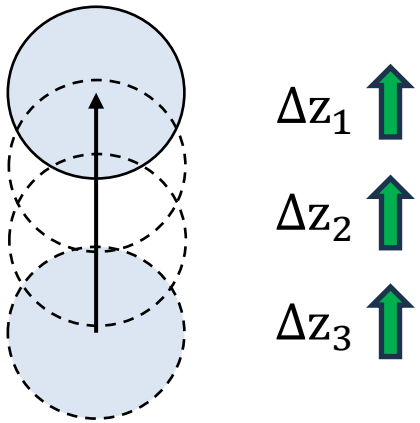

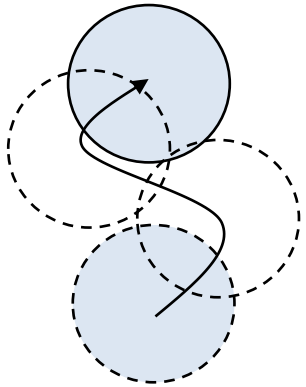

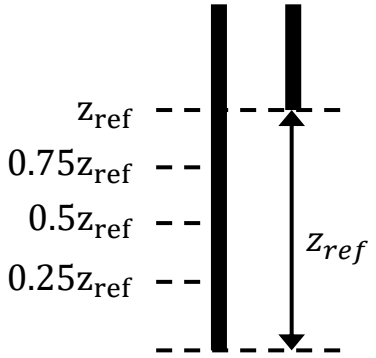

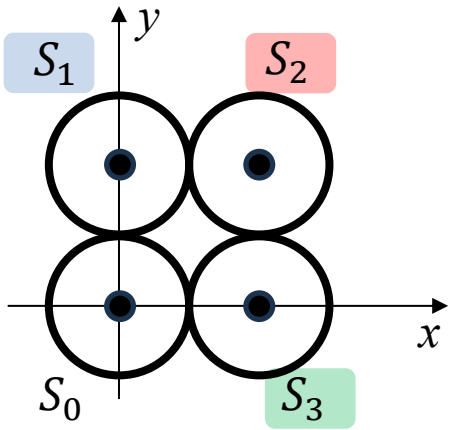

◎ **Configuration of the 4-sensor probes**

III. Evaluation results

◆ Measurement accuracy of bubble diameter(D_{32})

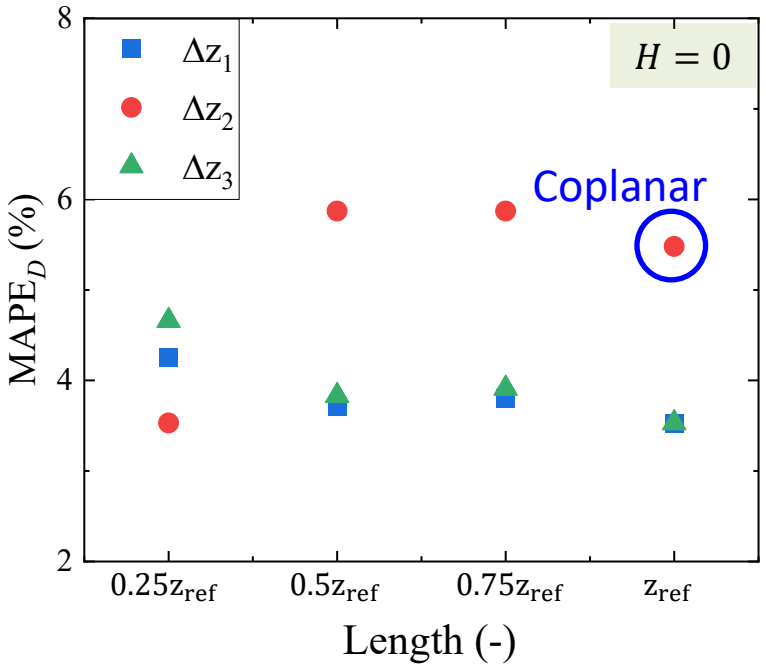

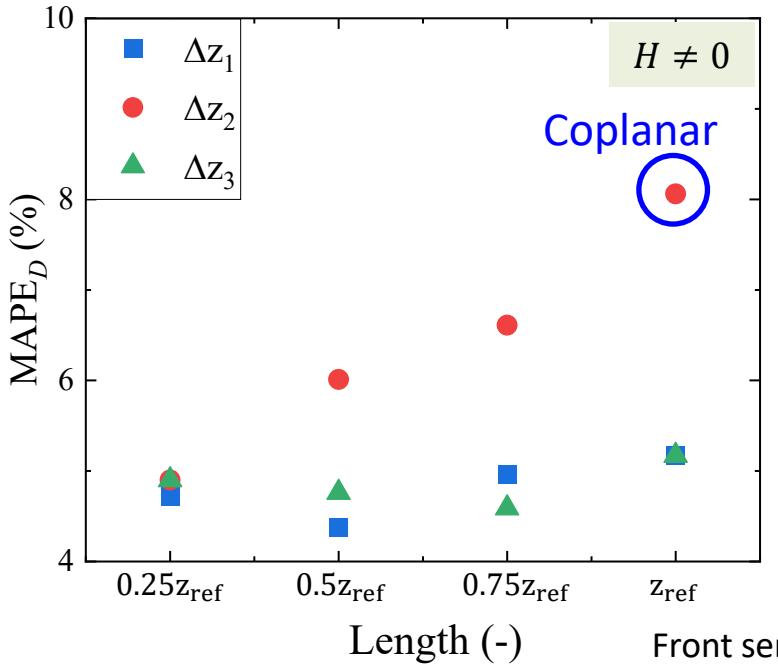

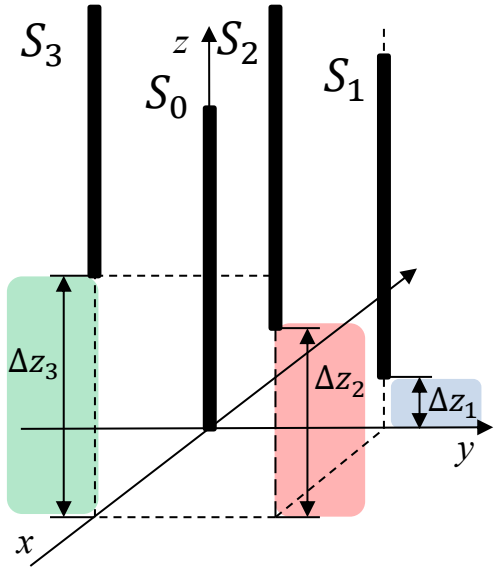

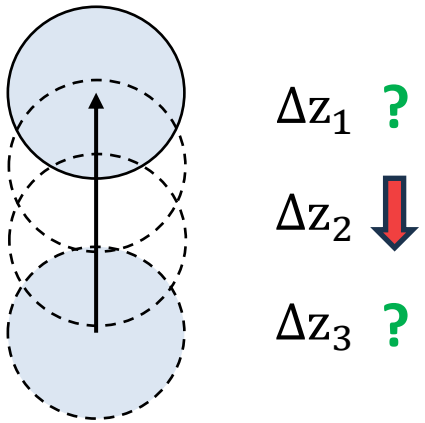

Δz_1 ?

Δz_2 ⇩

Δz_3 ?

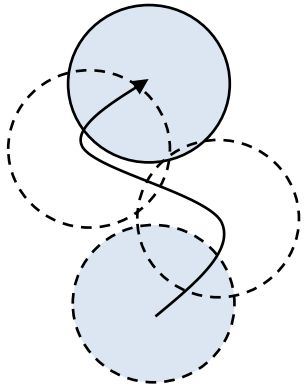

Δz_1 ?

Δz_2 ⇩

Δz_3 ?

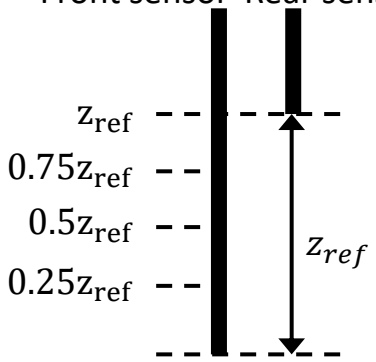

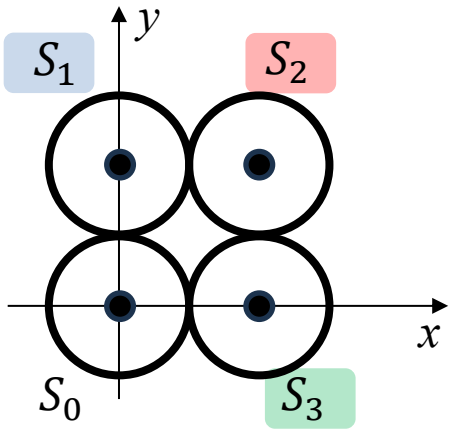

◎ **Configuration of the 4-sensor probes**

IV. Analyses of Displacement and Sensor-Failure

◆ Displacement(δ) sensitivity analysis

❖ $V_{distorted} = V_{\text{original}} + \boldsymbol{\delta_1 K}$

$$K \propto \left| \frac{V}{\Delta z_1 - \Delta z_2 + \Delta z_3} \right|$$

➢ $\boldsymbol{E_{V_b}, E_{D_{32}}} \propto \left| \frac{\mathbf{1}}{\Delta z_1 - \Delta z_2 + \Delta z_3} \right|$

$$\bar{a}_i \propto \frac{1}{\Omega} \sum_{j=1}^{N_{eff}} \left| \frac{1}{\vec{V}_{normal}} \right|$$

$$D_{32} = \frac{6\alpha}{\bar{a}_i}$$

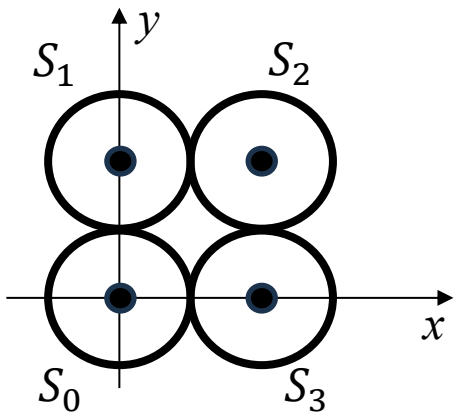

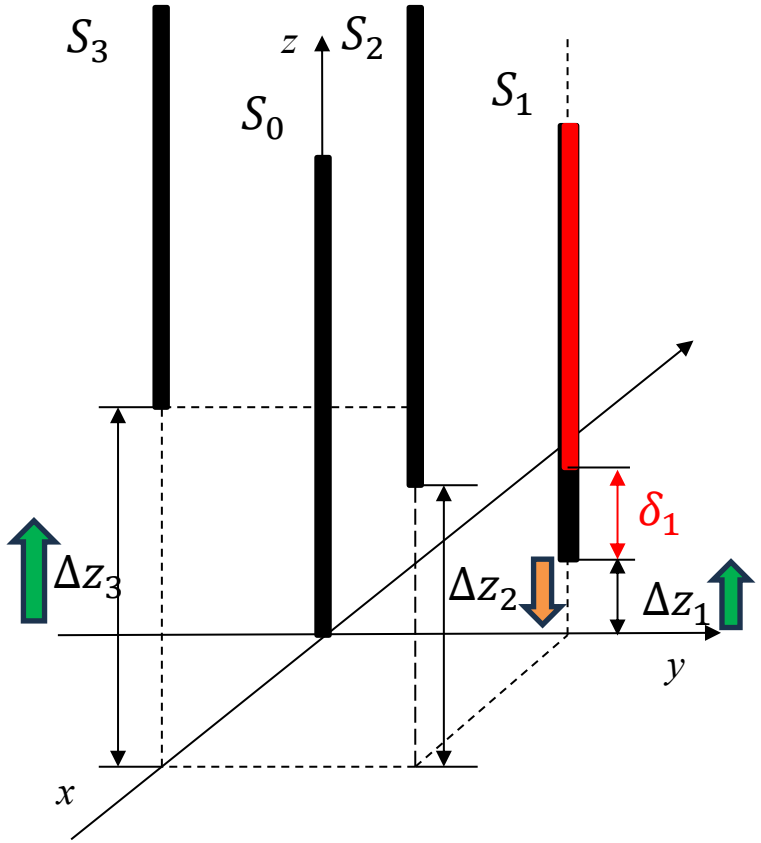

◎ Schematic of axial sensor-tip displacement

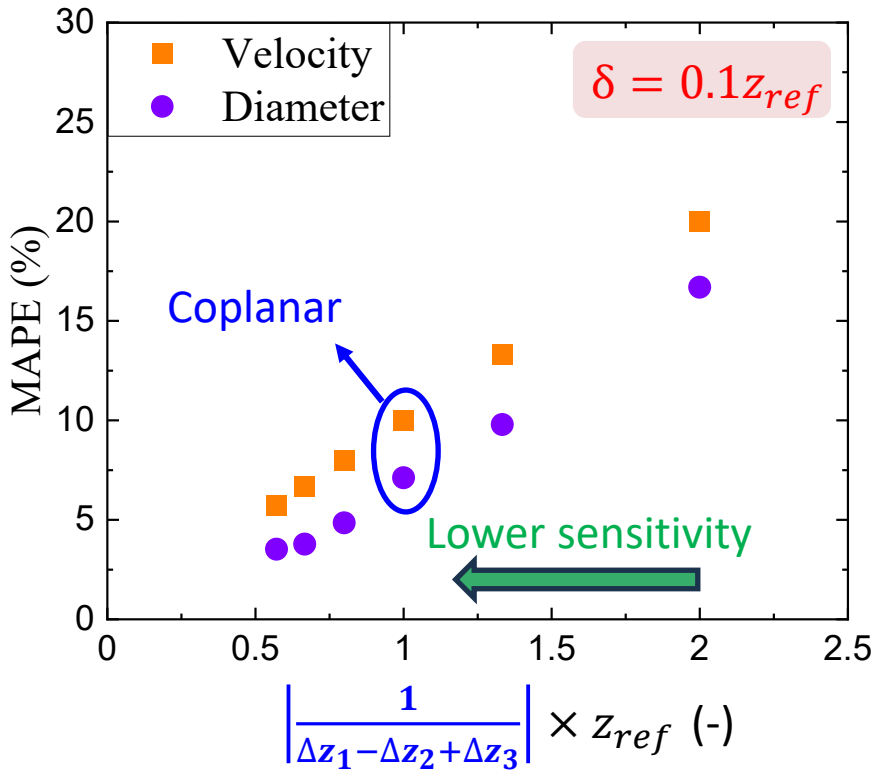

◎ Effect of displacement on V_b, D_{32} measurement

IV. Analyses of Displacement and Sensor-Failure

◆ Correction methods for single-rear sensor failure condition

1. 2-sensor method
   - Using 1 pair of front-rear sensor
   - $V_{2-S} = \frac{\Delta z}{\Delta t}$
2. Interpolated 4-sensor method
   - Assume $\Delta t \propto s$
   - $\Delta t_2^{interp} = \Delta t_1 + (s_2 - s_1)\frac{\Delta t_3 - \Delta t_1}{s_3 - s_1}$
3. Analytical 4-sensor method
   - Derived from V_{4-s} equation
   - $\Delta t_2 = -(z_1 - z_2 + z_3)/V_{4-S} + \Delta t_1 + \Delta t_3$
   - ➢ $\Delta t_2^{ana} = -(z_1 - z_2 + z_3)/\boldsymbol{V_{2-S}} + \Delta t_1 + \Delta t_3$
   - Estimation of V_{4-S}^{ana}

$$V_{4-s} = \frac{x_1(y_2z_3 - z_2y_3) - y_1(x_2z_3 - z_2x_3) + z_1(x_2y_3 - y_2x_3)}{\Delta t_1(x_2y_3 - y_2x_3) + \Delta t_2(x_3y_1 - x_1y_3) + \Delta t_3(x_1y_2 - y_1x_2)}$$

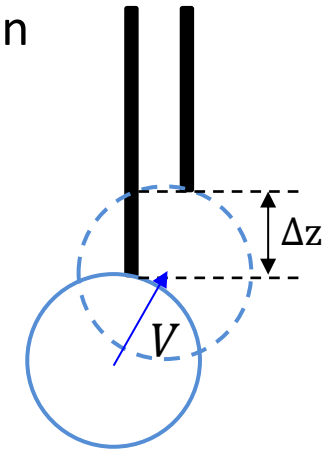

◎ **Measurement with 2-sensor probe**

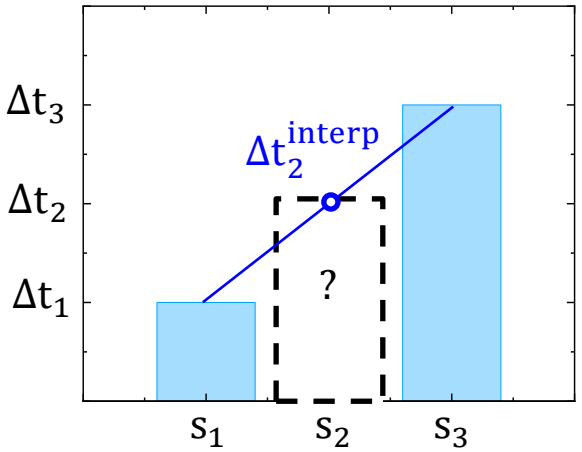

◎ **Reconstruction of Δt (interpolation)**

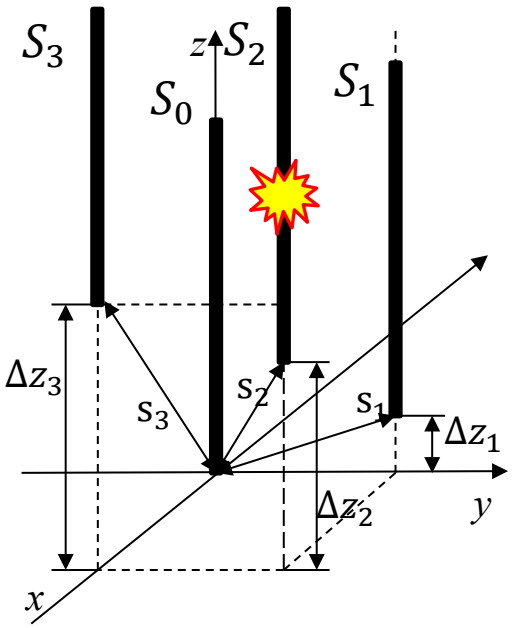

◎ **Sensor-fault situation**

IV. Analyses of Displacement and Sensor-Failure

◆ Evaluation result of sensor-failure correction methods (optimized 4-sensor configuration)

❖ Analytical 4-sensor method showed the lowest error (V_b:1.7%, D_{32}:10.3%)

$$\mathrm{MAPE} = \frac{1}{N}\sum_{i=1}^{N}\left|\frac{x_{\mathrm{correction}} - x_{4s}}{x_{4s}}\right| \times 100$$

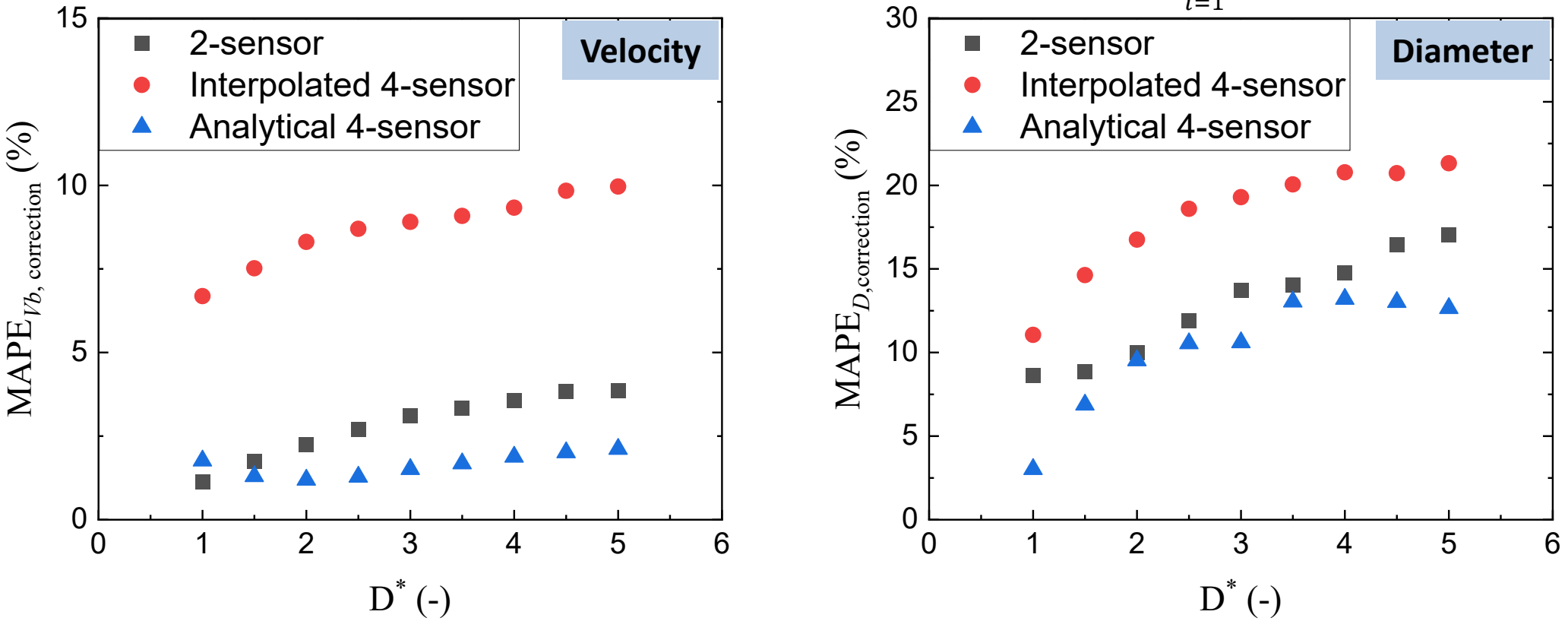

◎ **Evaluation results of correction methods**

V. Experimental validation using high-speed camera visualization

◆ Validation experiment using high-speed camera visualization

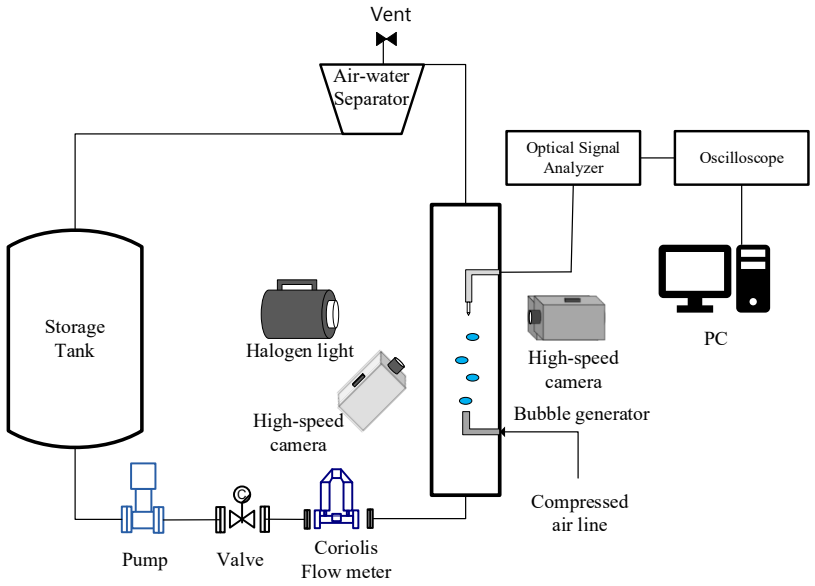

◎ Schematic of experimental loop

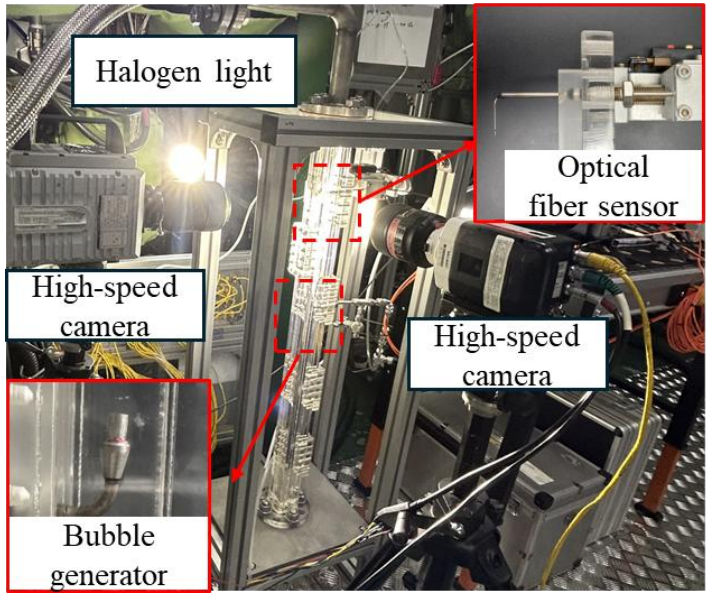

◎ Experimental setup

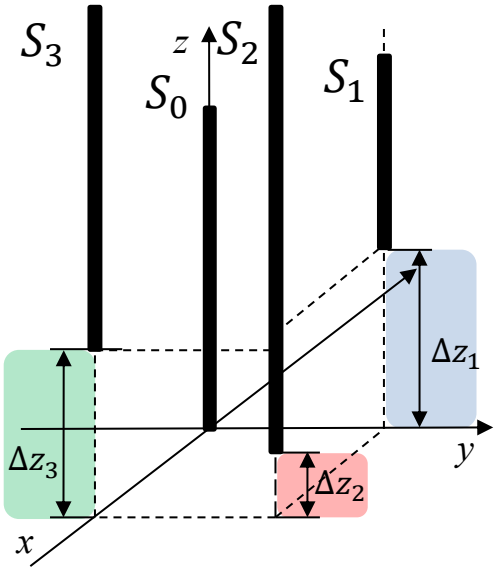

$\Delta z_1 = 1.9\text{mm}$
$\Delta z_2 = 0.5\text{mm}$
$\Delta z_3 = 1.5\text{mm}$

◎ 4-s OFP used for experiment

V. Experimental validation using high-speed camera visualization

◆ Results of validation experiment

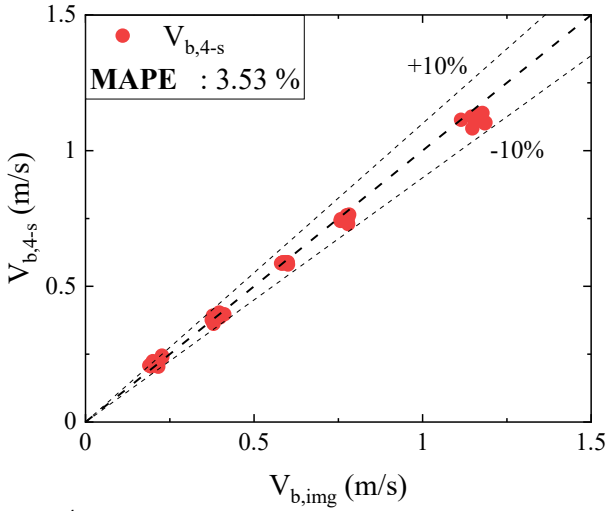

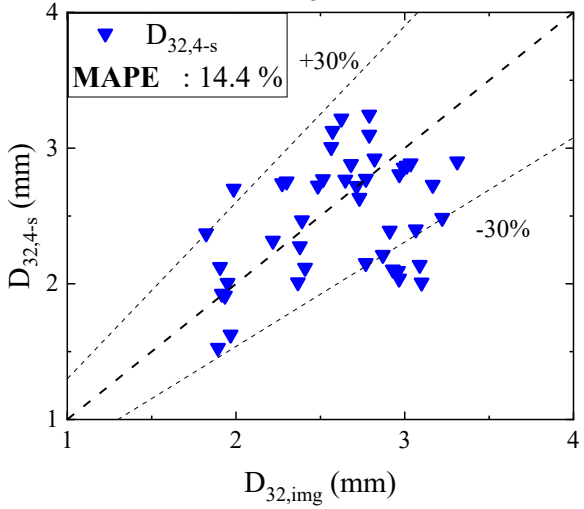

◎ Measurement results of V_b, D_{32}

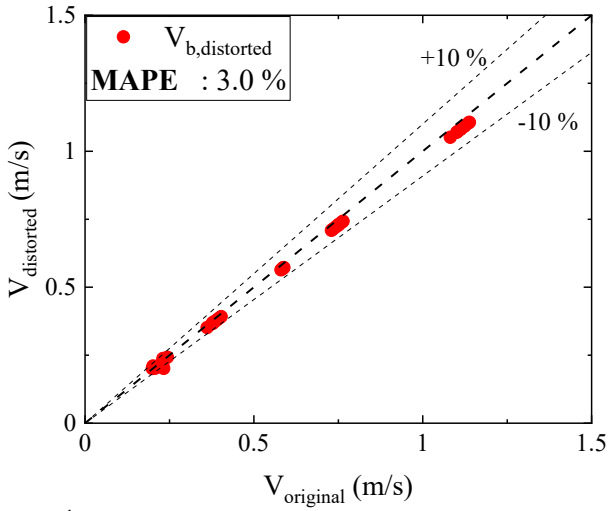

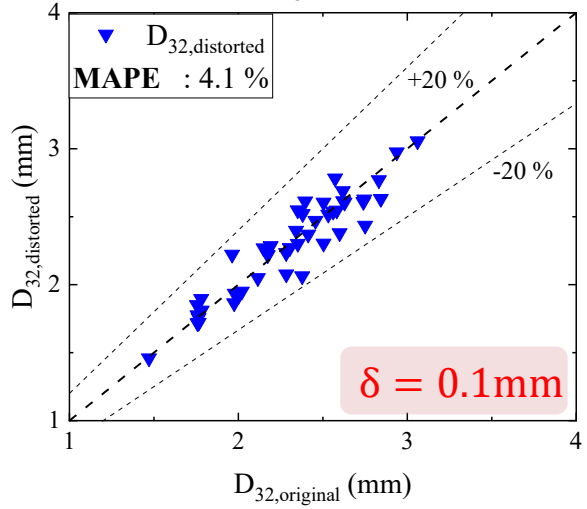

◎ Effect of displacement on measurement

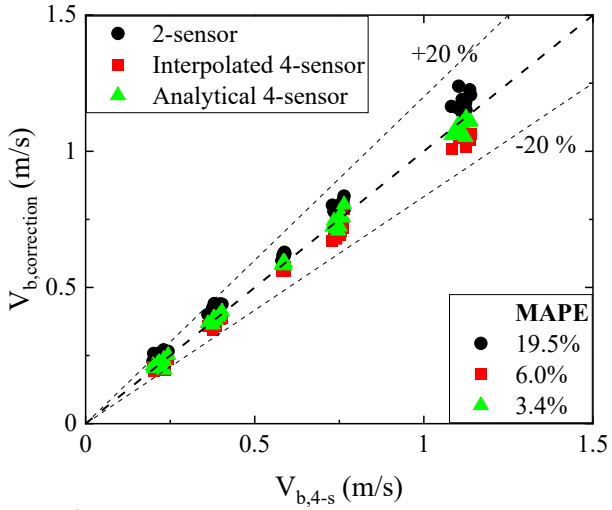

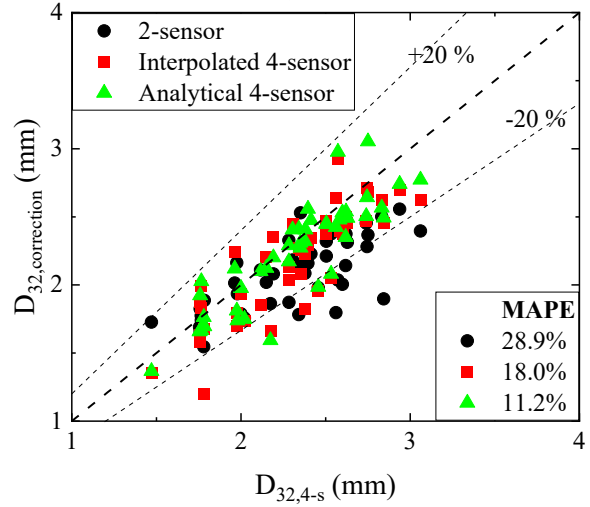

◎ Evaluation results of correction methods

VI. Conclusions

◆ Summary

- ❖ New 4-sensor probe configuration was proposed considering possible sensor damage
- ❖ An optimized 4-sensor array was identified to reduce displacement-induced error
- ❖ The analytical 4-sensor method is recommended for single rear-sensor failure conditions
- ❖ Simulation results were validated using high-speed camera visualization

◆ Future works

- ❖ Development of corrosion tolerance coating OFP sensor
- ❖ Application of developed multi-OFP methodology to high-pressure and temperature boiling water flow conditions

References

1) I. Kataoka, M. Ishii, and A. Serizawa, “Local formulation and measurements of interfacial area concentration in two-phase flow”, Int. J. Multiphase Flow, vol. 12, no. 4, pp. 505–529, 1986
2) S. T. Revankar and M. Ishii, “Theory and measurement of local interfacial area using a four sensor probe in two-phase flow”, Int. J. Heat Mass Transf., vol. 36, no. 12, pp. 2997–3007, 1993
3) J. M. Le Corre and M. Ishii, “Numerical evaluation and correction method for multi-sensor probe measurement techniques in two-phase bubbly flow”, Nucl. Eng. Des., vol. 216, no. 1–3, pp. 221–238, 2002
4) X. Shen, Y. Saito, K. Mishima, H. Nakamura, “Methodological improvement of an intrusive four-sensor probe for the multi-dimensional two-phase flow measurement”, Int. J. Multiphase Flow, vol. 31, no. 5, pp. 593–617, 2005
5) J. Moon, Y. Ko, S. G. Nam, J. J. Jeong, B. Yun, "Evaluation of the multi-sensor probe methods for the measurement of local bubble velocity and diameter", Int. Commun. Heat Mass Transf., vol. 135, 106146, 2022
6) S. Kim, X. Y. Fu, X. Wang, and M. Ishii, “Development of the miniaturized four-sensor conductivity probe and the signal processing scheme,” Int. J. Heat Mass Transfer, 43(22), 4101–4118, 2000

Q & A

Thank you for attention

Appendix

◆ Evaluation results

$D^* = 0.1 - 5.0$ (250,000 bubbles × 50cases)

	①	②	③	④
④	0.23%	0.14%	0.05%	0.03%
③	0.27%	0.17%	0.07%	0.04%
②	0.33%	0.20%	0.11%	0.11%
①	0.30%	0.21%	0.26%	0.50%

Δz_3

Δz_2

< Δz_1 = ④ fixed >

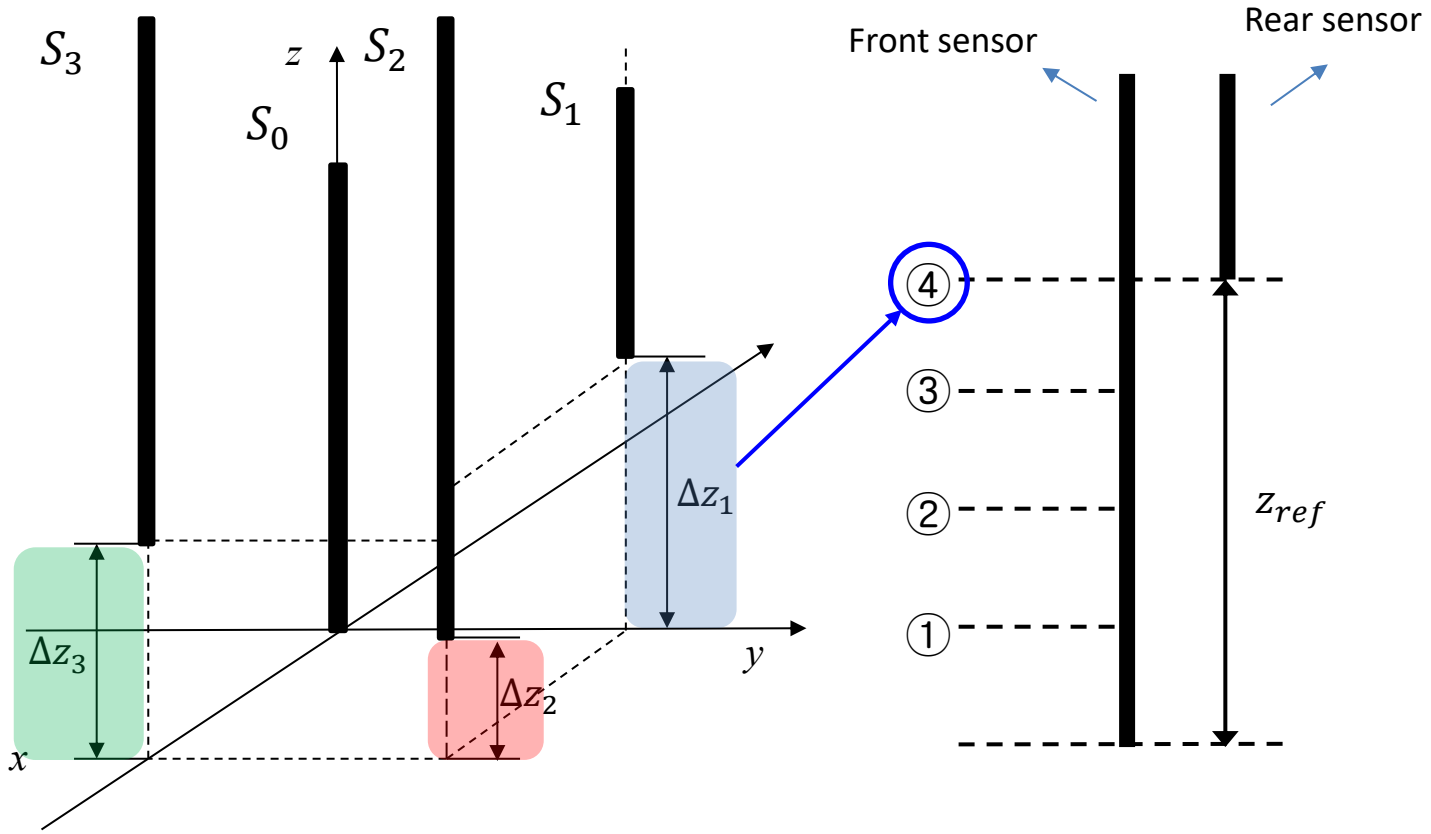

◎ Configuration of the 4-sensor probes

Appendix

◆ Measurement accuracy of bubble velocity

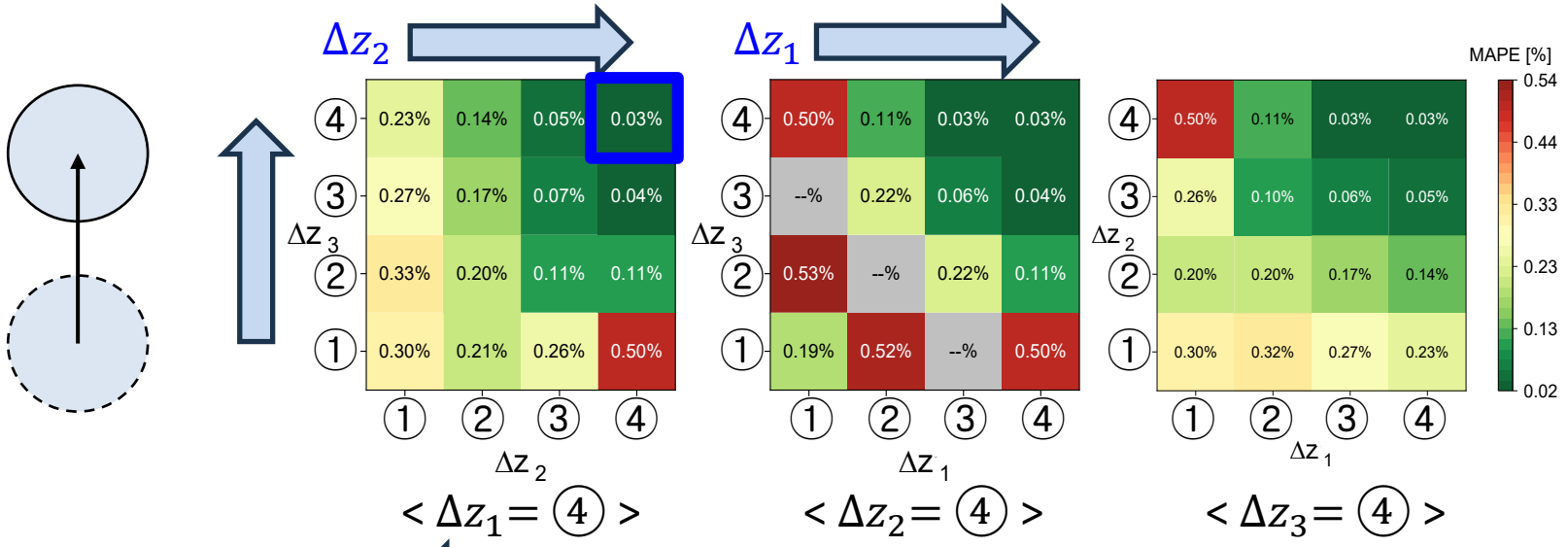

$< \Delta z_1 = ④ >$ $< \Delta z_2 = ④ >$ $< \Delta z_3 = ④ >$

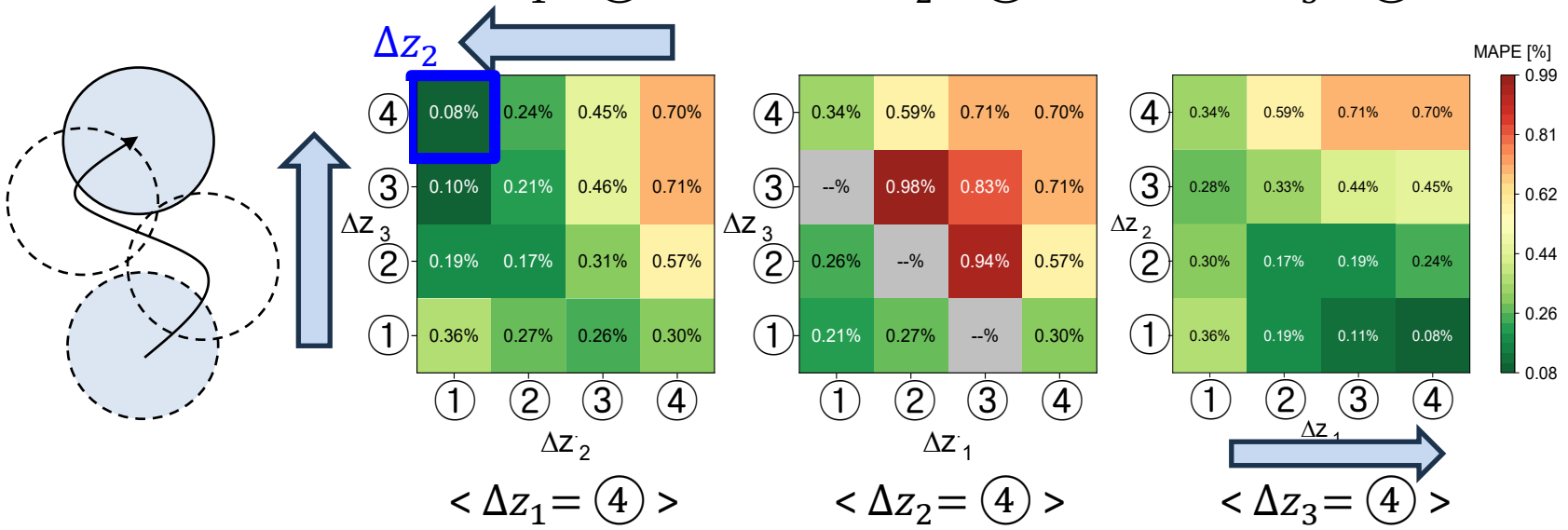

$< \Delta z_1 = ④ >$ $< \Delta z_2 = ④ >$ $< \Delta z_3 = ④ >$

Array	$(\Delta z_1, \Delta z_2, \Delta z_3)$	$E_{H_{max}=0.0}$	$E_{H_{max}=0.2}$
Coplanar	(4,4,4)	0.03%	0.70%
V-1	(4,1,4)	0.23%	0.08%

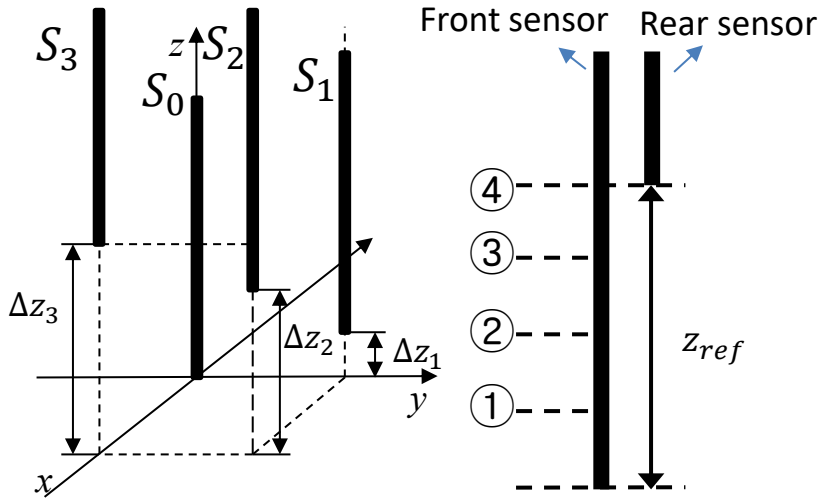

◎ Configuration of the 4-sensor probes

Appendix

◆ Measurement accuracy of Sauter mean diameter(D_{32})

❖ $H_{max} = 0.0$

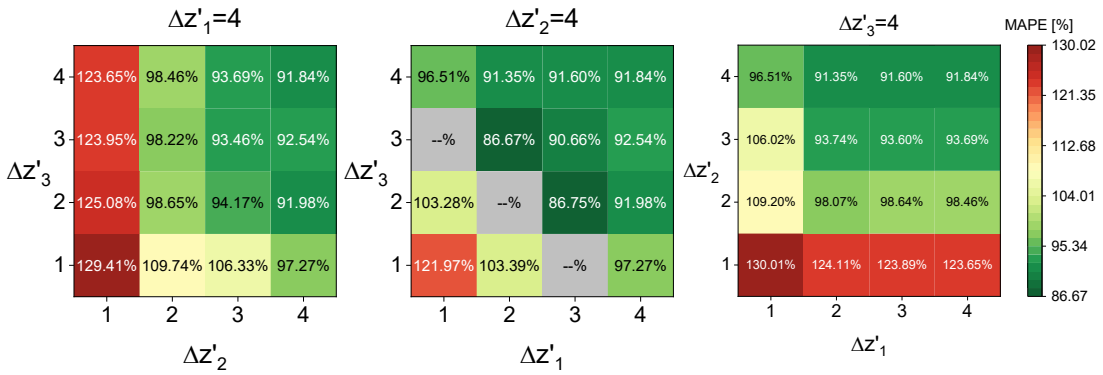

< Kataoka et al. ($E_{min} = 86.67\%$) >

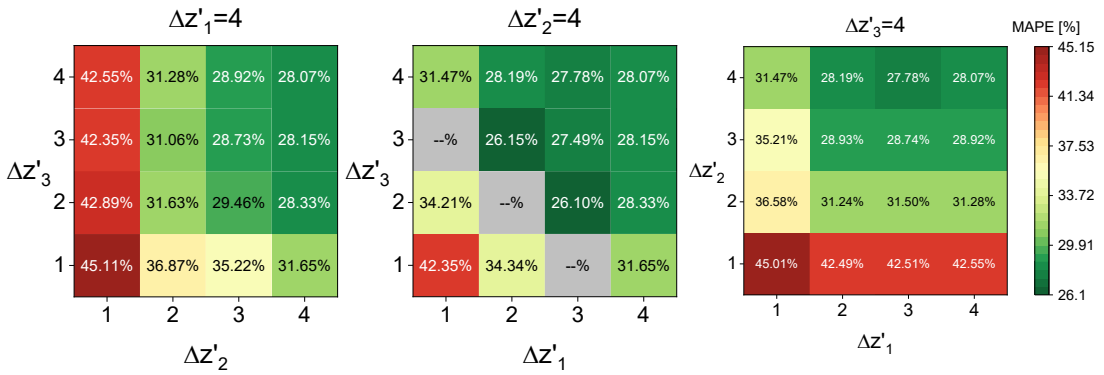

< Revankar & Ishii ($E_{min} = 26.10\%$) >

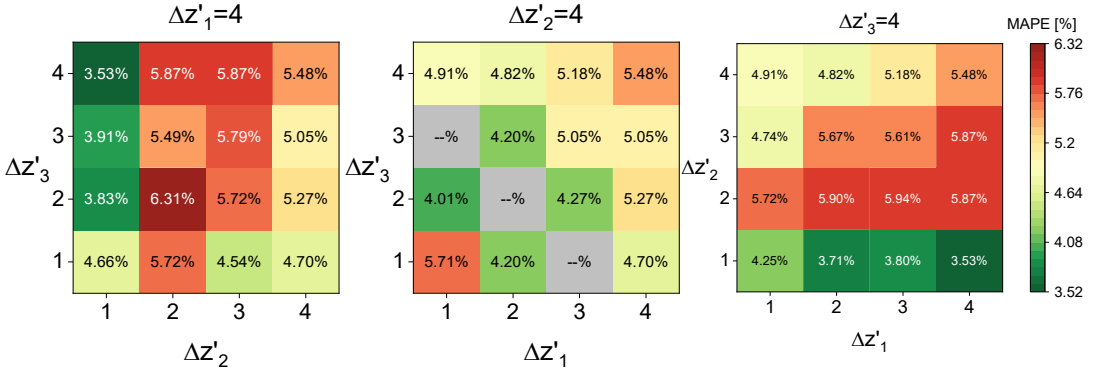

< Le Corre & Ishii ($E_{min} = 3.53\%$) >

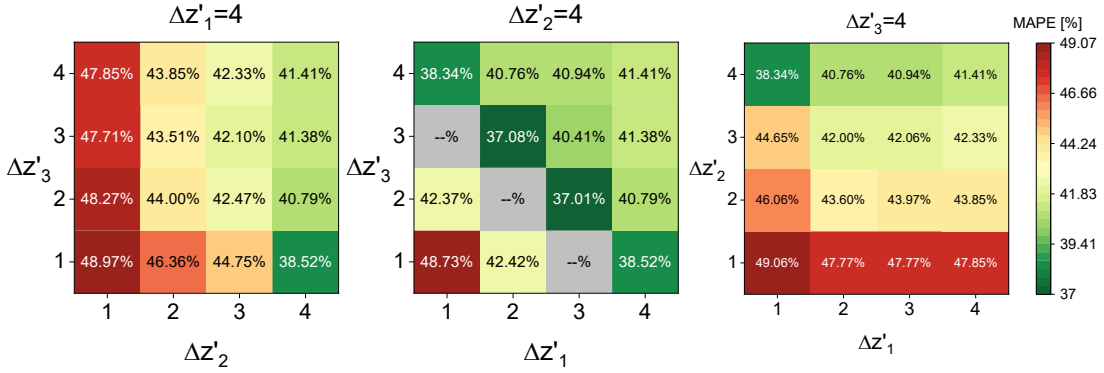

< Kim et al. ($E_{min} = 37.01\%$) >

Appendix

◆ Measurement accuracy of Sauter mean diameter(D_{32})

❖ $H_{max} = 0.2$

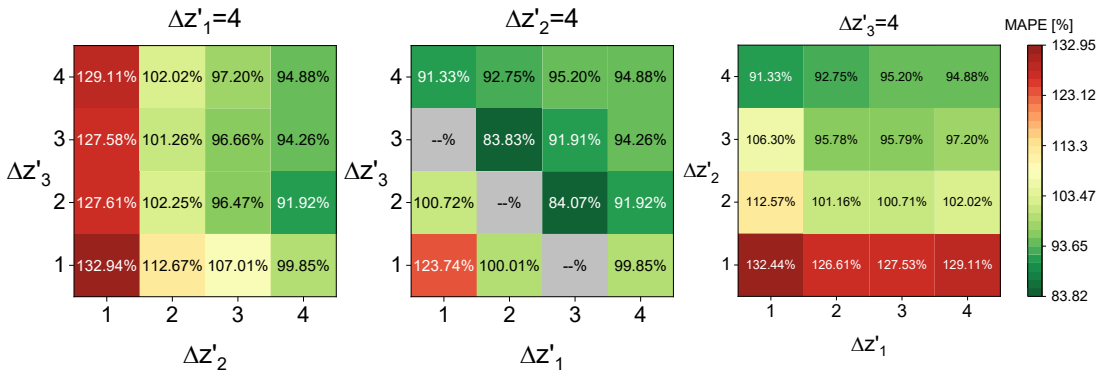

< Kataoka et al. ($E_{min} = 83.83\%$) >

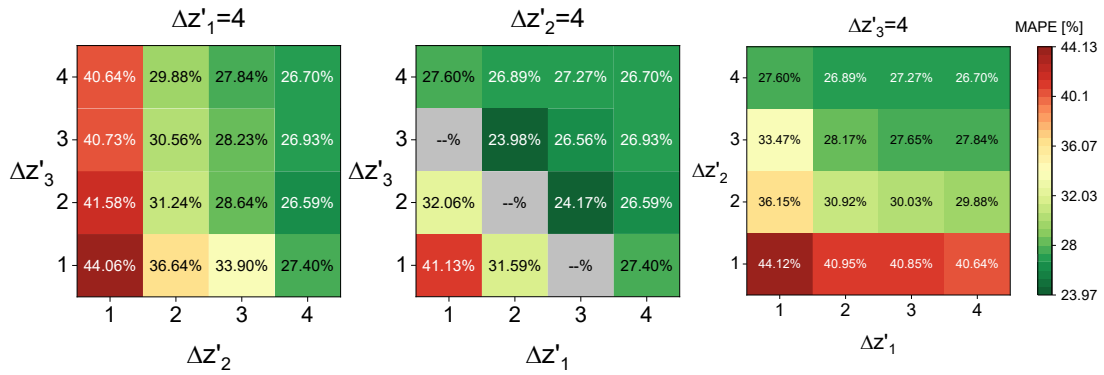

< Revankar & Ishii ($E_{min} = 23.98\%$) >

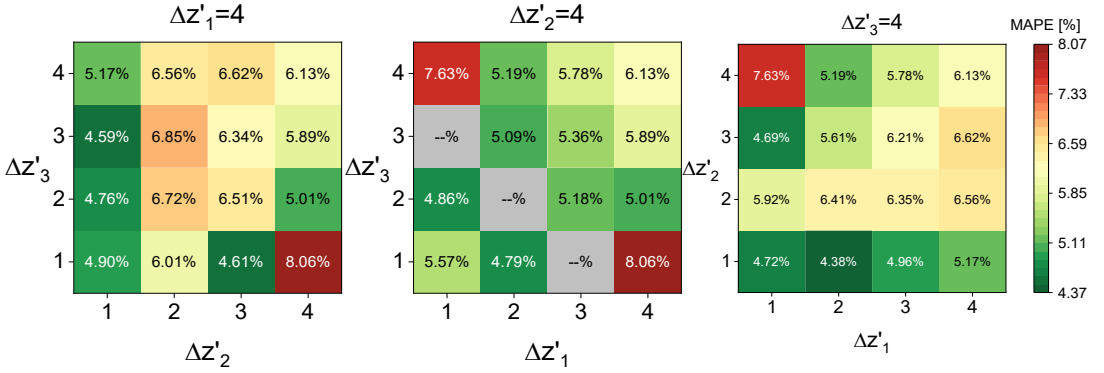

< Le Corre & Ishii ($E_{min} = 4.38\%$) >

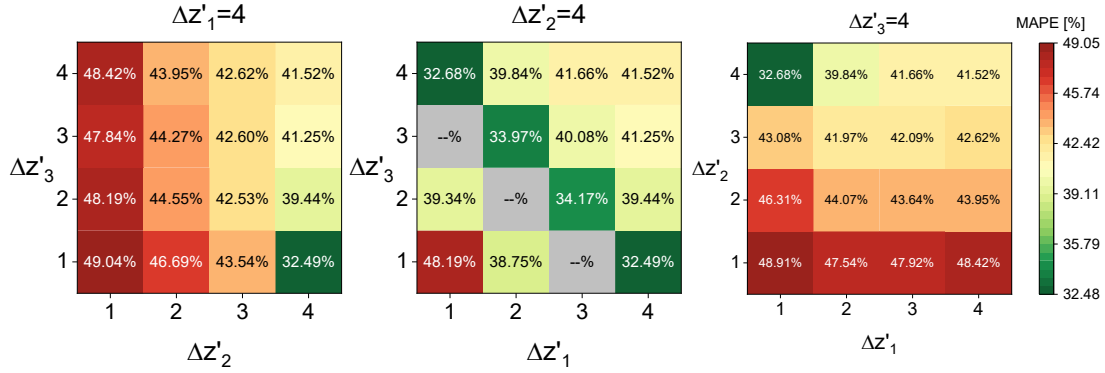

< Kim et al. ($E_{min} = 32.49\%$) >

Appendix

◆ Existing IAC measurement models

Researcher	IAC measurement model	Features
Kataoka et al.	$\bar{a}_{\mathrm{i}} = \frac{1}{\Omega}\sum_{j=1}^{N_{\mathrm{eff}}} \left\lvert \frac{1}{\vec{V}_{\mathrm{normal,j}}} \right\rvert$	Did not consider velocity fluctuation and bubble size distribution Errors caused by missing bubbles
Revankar & Ishii	$\bar{a}_{\mathrm{i}} = \frac{1}{\Omega}\sum_{j=1}^{N_{\mathrm{eff}}} \left\lvert \frac{1}{\vec{V}_{\mathrm{normal,j}}} \right\rvert + \frac{\tau_b}{\Omega}\frac{l_d}{s_p}$	Accounted for missing bubbles using probe geometry (l_d, s_p) and bubble residence time (τ_b)
Le Corre & Ishii	$\bar{a}_{\mathrm{i}} = \frac{1}{\Omega}\sum_{j=1}^{N_{\mathrm{eff}}} \left\lvert \frac{1}{\vec{V}_{\mathrm{normal,j}}} \right\rvert \frac{1}{\sqrt{1-\sqrt{2.4 r_{\mathrm{N}} - 1.5 r_{\mathrm{N}}^2}}}$	Divided signals into missing and effective signals Used the ratio of missing signals to total signals (r_{N}) for correction
Kim et al.	$\bar{a}_{\mathrm{i}} = (\bar{a}_{\mathrm{i}})_{\mathrm{f,eff}}\left(\frac{N_{\mathrm{tot}}}{N_{\mathrm{f,eff}}}\right) + (\bar{a}_{\mathrm{i}})_{\mathrm{r,eff}}\left(\frac{N_{\mathrm{tot}}}{N_{r,\mathrm{eff}}}\right)$	Divided average $\bar{a}_{\mathrm{i}}$ values into front and rear interface

Appendix

◆ Measurement accuracy of bubble diameter(D_{32})

IAC Model	Best array $(\Delta z_1, \Delta z_2, \Delta z_3)$	$E_{H_{max}=0.0}$ [%]	$E_{H_{max}=0.2}$ [%]	E_{avg} [%]
Kataoka et al.	(2,4,3)	86.7	83.8	**85.3**
Revankar & Ishii	(2,4,3)	26.2	24.0	**25.1**
Le Corre & Ishii	(2,1,4)	3.7	4.4	**4.0**
	(4,1,3)	3.9	4.6	**4.3**
Kim et al.	(1,4,4)	38.5	32.5	**35.5**

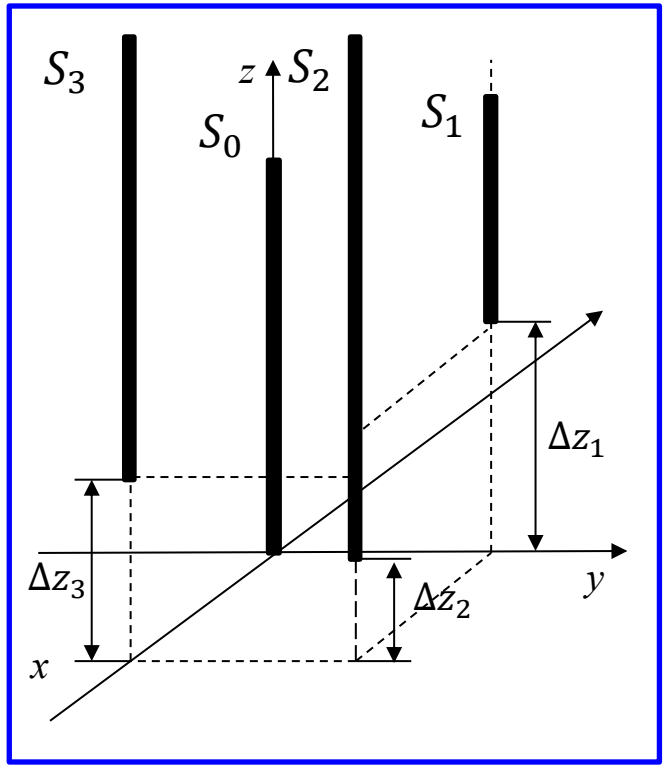

➢ Le Corre & Ishii model showed the lowest D_{32} error

Appendix

◆ Detail of displacement robustness analysis

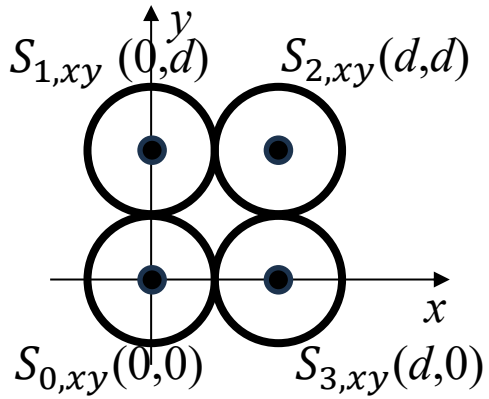

- $V_{4-s,original} = \frac{|\vec{V}_{normal}|}{cos\eta_{zv}} = \frac{A_0}{A_3} = \frac{x_1(y_2z_3-z_2y_3)-y_1(x_2z_3-z_2x_3)+z_1(x_2y_3-y_2x_3)}{x_1\left(y_2\frac{S_3}{V_3}-y_3\frac{S_2}{V_2}\right)-y_1\left(x_2\frac{S_3}{V_3}-x_3\frac{S_2}{V_2}\right)+t_1(x_2y_3-y_2x_3)}$

- $V_{4-s,S1\ distorted} = \frac{x_1(y_2z_3-z_2y_3)-y_1(x_2z_3-z_2x_3)+(z_1+\delta)(x_2y_3-y_2x_3)}{x_1\left(y_2\frac{S_3}{V_3}-y_3\frac{S_2}{V_2}\right)-y_1\left(x_2\frac{S_3}{V_3}-x_3\frac{S_2}{V_2}\right)+t_1(x_2y_3-y_2x_3)}$

$$= V_{4-s,original} + \delta \boxed{\frac{(x_2y_3 - y_2x_3)}{x_1\left(y_2\frac{S_3}{V_3} - y_3\frac{S_2}{V_2}\right) - y_1\left(x_2\frac{S_3}{V_3} - x_3\frac{S_2}{V_2}\right) + t_1(x_2y_3 - y_2x_3)}} = K_1$$

- $K_1 = \frac{(x_2y_3-y_2x_3)}{x_1\left(y_2\frac{S_3}{V_3}-y_3\frac{S_2}{V_2}\right)-y_1\left(x_2\frac{S_3}{V_3}-x_3\frac{S_2}{V_2}\right)+t_1(x_2y_3-y_2x_3)} = \frac{x_2y_3-y_2x_3}{\frac{S_1}{V_1}(x_2y_3-y_2x_3)+\frac{S_2}{V_2}(x_3y_1-x_1y_3)+\frac{S_3}{V_3}(x_1y_2-y_1x_2)}$
  - $x_1, y_3 = 0$
  - $x_2, x_3, y_1, y_2 = \mathrm{d}$

➢ $K_1 = \frac{-\mathrm{d}^2}{-\mathrm{d}^2\frac{S_1}{V_1}+\mathrm{d}^2\frac{S_2}{V_2}-\mathrm{d}^2\frac{S_3}{V_3}} = \frac{1}{\frac{S_1}{V_1}-\frac{S_2}{V_2}+\frac{S_3}{V_3}} = \frac{V}{S_1-S_2+S_3}, (V_1 \approx V_2 \approx V_3 \approx V)$

Appendix

◆ Detail of analytical method derivation

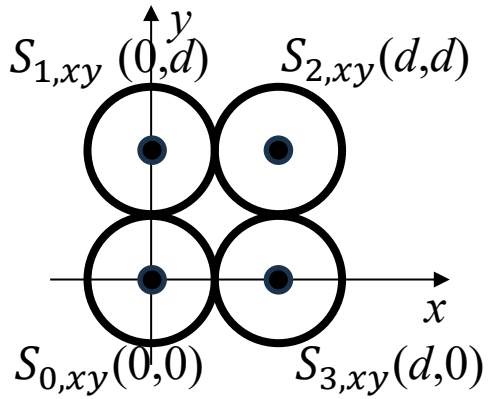

- $V_{4-s,original} = \frac{|\vec{V}_{normal}|}{cos\eta_{zv}} = \frac{A_0}{A_3} = \frac{x_1(y_2z_3-z_2y_3)-y_1(x_2z_3-z_2x_3)+z_1(x_2y_3-y_2x_3)}{x_1\left(y_2\frac{S_3}{V_3}-y_3\frac{S_2}{V_2}\right)-y_1\left(x_2\frac{S_3}{V_3}-x_3\frac{S_2}{V_2}\right)+t_1(x_2y_3-y_2x_3)}$

- $V_{4-s,S1\ distorted} = \frac{x_1(y_2z_3-z_2y_3)-y_1(x_2z_3-z_2x_3)+(z_1+\delta)(x_2y_3-y_2x_3)}{x_1\left(y_2\frac{S_3}{V_3}-y_3\frac{S_2}{V_2}\right)-y_1\left(x_2\frac{S_3}{V_3}-x_3\frac{S_2}{V_2}\right)+t_1(x_2y_3-y_2x_3)}$

$$= V_{4-s,original} + \delta\frac{(x_2y_3 - y_2x_3)}{x_1\left(y_2\frac{S_3}{V_3} - y_3\frac{S_2}{V_2}\right) - y_1\left(x_2\frac{S_3}{V_3} - x_3\frac{S_2}{V_2}\right) + t_1(x_2y_3 - y_2x_3)} = K_1$$

- $K_1 = \frac{(x_2y_3-y_2x_3)}{x_1\left(y_2\frac{S_3}{V_3}-y_3\frac{S_2}{V_2}\right)-y_1\left(x_2\frac{S_3}{V_3}-x_3\frac{S_2}{V_2}\right)+t_1(x_2y_3-y_2x_3)} = \frac{x_2y_3-y_2x_3}{\frac{S_1}{V_1}(x_2y_3-y_2x_3)+\frac{S_2}{V_2}(x_3y_1-x_1y_3)+\frac{S_3}{V_3}(x_1y_2-y_1x_2)}$
  - $x_1, y_3 = 0$
  - $x_2, x_3, y_1, y_2 = \mathrm{d}$

➢ $K_1 = \frac{-\mathrm{d}^2}{-\mathrm{d}^2\frac{S_1}{V_1}+\mathrm{d}^2\frac{S_2}{V_2}-\mathrm{d}^2\frac{S_3}{V_3}} = \frac{1}{\frac{S_1}{V_1}-\frac{S_2}{V_2}+\frac{S_3}{V_3}} = \frac{V}{S_1-S_2+S_3}, (V_1 \approx V_2 \approx V_3 \approx V)$

Appendix

◆ Displacement(δ) sensitivity analysis

❖ $V_{distorted} = \frac{x_1(y_2z_3 - z_2y_3) - y_1(x_2z_3 - z_2x_3) + (z_1 + \boldsymbol{\delta_1})(x_2y_3 - y_2x_3)}{\Delta t_1(x_2y_3 - y_2x_3) + \Delta t_2(x_3y_1 - x_1y_3) + \Delta t_3(x_1y_2 - y_1x_2)} = V_{\text{original}} + \boldsymbol{\delta_1 K}$ (Abs. Error)

$K \propto \left|\frac{V}{z_1 - z_2 + z_3}\right|$

➢ Rel. Error $\boldsymbol{E_{V_b}, E_{D_{32}}} \propto \left|\frac{\mathbf{1}}{\boldsymbol{z_1 - z_2 + z_3}}\right|$

$\bar{a}_i \propto \frac{1}{\Omega}\sum_{j=1}^{N_{eff}} \left|\frac{1}{\vec{V}_{normal}}\right|$

$D_{32} = \frac{6\alpha}{\bar{a}_i}$

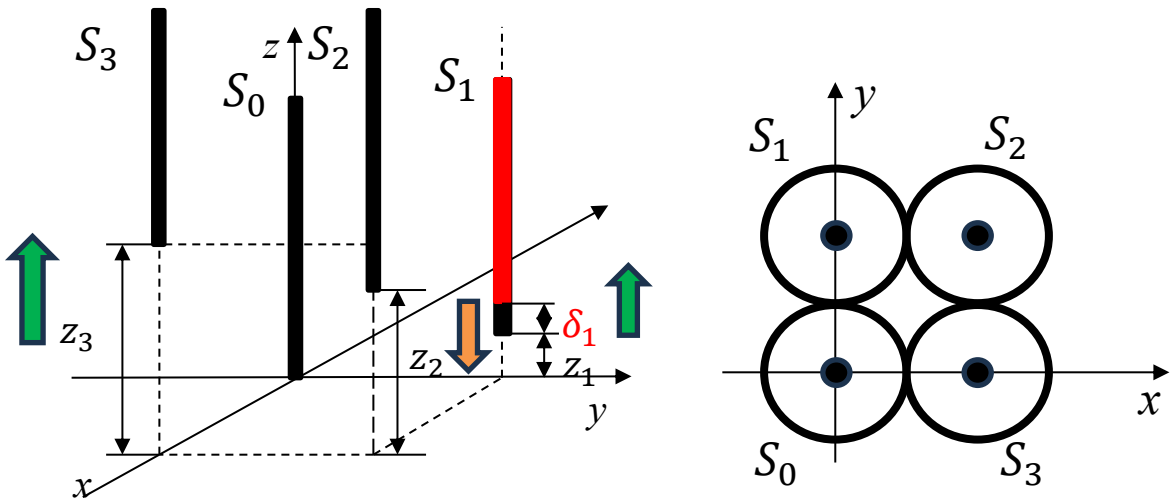

◎ Configuration of the 4-sensor probes

$$\text{MAPE} = \frac{1}{N}\sum_{i=1}^{N}\left|\frac{x_{distorted} - x_{original}}{x_{original}}\right| \times 100$$

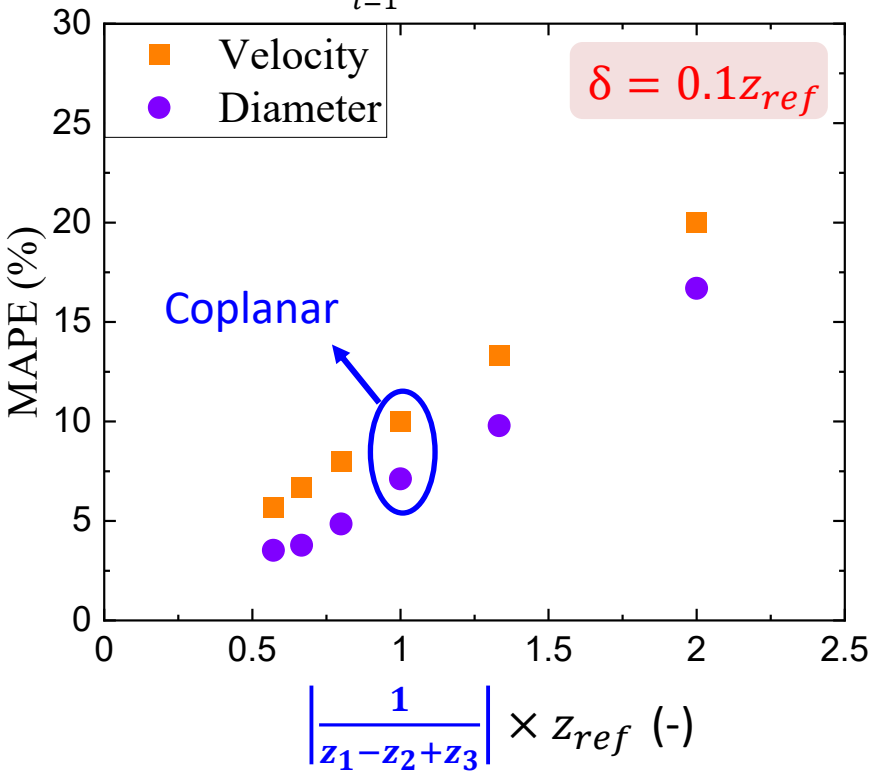

◎ Effect of displacement on V_b, D_{32} measurement